

s-wave Superconductivity due to Suhl-Kondo Mechanism in $\text{Na}_x\text{CoO}_2 \cdot y\text{H}_2\text{O}$: Effect of Coulomb Interaction and Trigonal Distortion

Keiji YADA

Toyota Physical and Chemical Research Institute, Nagakute-cho, Aichi-gun 480-1192, Japan.

Hiroshi KONTANI

Department of Physics, Nagoya University, Furo-cho, Nagoya 464-8602, Japan.

To study the electron-phonon mechanism of superconductivity in $\text{Na}_x\text{CoO}_2 \cdot y\text{H}_2\text{O}$, we perform semiquantitative analysis of the electron-phonon interaction (EPI) between relevant optical phonons (breathing and shear phonons) and t_{2g} electrons (a_{1g} and e'_g electrons) in the presence of trigonal distortion. We consider two kinds of contributions to the EPI; the EPI originating from the Coulomb potential of O ions and that originating from the d - p transfer integral between Co and O in CoO_6 octahedron. We find that the EPI for shear phonons, which induces the interorbital hopping of electrons, is large in $\text{Na}_x\text{CoO}_2 \cdot y\text{H}_2\text{O}$ because of the trigonal distortion of CoO_2 layer. For this reason, T_c for s -wave pairing is prominently enlarged owing to interorbital hopping of Cooper pairs induced by shear phonons, even if the top of e'_g electron band is close to but below the Fermi level as suggested experimentally. This mechanism of superconductivity is referred to as the valence-band Suhl-Kondo (SK) mechanism. Since the SK mechanism is seldom damaged by the Coulomb repulsion, s -wave superconductivity is realized irrespective of large Coulomb interaction $U \sim 5$ eV at Co sites. We also study the oxygen isotope effect on T_c , and find that it becomes very small due to strong Coulomb interaction. Finally, we discuss the possible mechanism of anisotropic s -wave superconducting state in $\text{Na}_x\text{CoO}_2 \cdot y\text{H}_2\text{O}$, resulting from the coexistence of strong EPI and the antiferromagnetic fluctuations.

PACS numbers: 74.20.-z, 74.20.Mn, 71.10.Fd

I. INTRODUCTION

Superconducting layered cobalt oxide $\text{Na}_x\text{CoO}_2 \cdot y\text{H}_2\text{O}$ ($x \sim 0.35$, $y \sim 1.3$) with $T_c \sim 4.5$ K has attracted considerable attention since it is the first discovered superconducting cobaltates [1]. The parent compound Na_xCoO_2 reveals rich phase diagram depending on the Na content x [2]. Yokoi *et al.* have found that the electronic state of Na_xCoO_2 drastically changes at the boundary $x \sim 0.6$ [3]. For example, the uniform magnetic susceptibility decreases with decreasing temperature for $x \leq 0.6$, while it shows a Curie-Weiss-like behavior for $x \geq 0.6$ [3, 4]. The quasiparticle spectra in photoemission spectroscopy [5] and optical conductivity in infrared spectroscopy [6] also decrease with decreasing temperature for $x \leq 0.6$. It is noteworthy that these "weak pseudogap" behavior is also observed in the normal state of superconducting $\text{Na}_x\text{CoO}_2 \cdot y\text{H}_2\text{O}$. In the superconducting state of $\text{Na}_x\text{CoO}_2 \cdot y\text{H}_2\text{O}$, a sizable decrease of the Knight shift is observed independently of the direction of magnetic field, which indicates that the spin singlet superconductivity is realized [7, 8, 9]. A power law behavior in $1/T_1T$ suggests the large anisotropy in superconducting gap, like a line-node state [10, 11, 12]. On the other hand, the decreasing rate of T_c due to non-magnetic impurities in this system is much smaller than that of the d -wave superconductor, and it is as small as that of s -wave superconductor MgB_2 [13]. This fact suggests that the sign of the superconducting gap function is unchanged everywhere.

In considering the mechanism and the pairing symmetry of superconductor, the Fermi surface (FS) topol-

ogy gives the most important information. The FSs in Na_xCoO_2 are composed of t_{2g} -orbitals of Co ion, which split into the a_{1g} -orbital and twofold e'_g -orbitals due to crystalline electric field. The first principle calculation based on local density approximation (LDA) [14] had predicted the presence of six small hole pockets due to the e'_g bands near the K-points, in addition to a cylindrical FS due to the a_{1g} band around Γ -point. However, such e'_g hole pockets are not observed in ARPES measurements, since the e'_g bands are completely below the Fermi level independently of the Na content [15]. They are also not observed in the bulk-sensitive ARPES using soft X-ray that has longer escape depth [16]. Moreover, the shape of FS does not change by the intercalation of water [17]. We stress that an estimated specific heat coefficient γ_{est} using the a_{1g} Fermi velocity given by ARPES [18] is consistent with experimental value $\gamma \sim 11$ mJ/mol K². If there were e'_g hole pockets, the realized γ should be about 3 times greater than the experimental value because of the large density of states (DOS) given by the e'_g hole pockets, as pointed out in Ref. [19]. This fact reinforces the observation by ARPES measurements.

To determine the FS topology theoretically, present authors have studied the normal electronic state of Na_xCoO_2 based on the fluctuation-exchange (FLEX) approximation, which is a self-consistent spin-fluctuation theory [19]. In the FLEX approximation, experimentally observed weak pseudogap behaviors in the DOS and magnetic susceptibility appear when the top of the e'_g -band is slightly below the Fermi level, that is, the e'_g hole pockets are absent. We found that the weak pseudogap behav-

iors originate from (i) antiferromagnetic (AF) fluctuations due to Coulomb interaction, and (ii) large DOS of the e'_g hole pockets that exist slightly below the Fermi level. When e'_g hole pockets are present, on the other hand, ferromagnetic fluctuations are induced by the e'_g hole pockets, and "anti-pseudogap behavior" appears in the DOS [19]. These results are highly inconsistent with experiments. Therefore, Na_xCoO_2 should have a single cylindrical FS around the Γ -point.

After the discovery of $\text{Na}_x\text{CoO}_2 \cdot y\text{H}_2\text{O}$, various kinds of superconducting states had been proposed [20, 21, 22]. In particular, possibility of triplet superconducting state due to Coulomb interaction were investigated based on the FS with e'_g hole pockets, by using perturbational theory [23, 24] or FLEX approximation [25, 26]. However, successive experimental efforts had revealed that e'_g hole pockets are absent [17], and singlet superconducting state is realized [7, 8]. Moreover, ferromagnetic fluctuations are not observed by inelastic neutron diffraction in a superconducting single crystal [27]. Therefore, we now have to find a mechanism of singlet superconducting based on the large a_{1g} FS around the Γ point. If e'_g hole pockets are absent, however, the expected magnetic fluctuations seem to be too small to realize unconventional superconductivity [25]. Considering the small impurity effect on T_c [13], we should examine the possibility of superconductivity caused by the electron-phonon interaction (EPI). In fact, several experimental studies show the presence of considerable electron-boson coupling in Na_xCoO_2 : For example, the kink structure was observed in the quasiparticle spectrum in ARPES measurement at $\omega \sim 600 \text{ cm}^{-1}$ [16]. In addition, ω -dependence of scattering rate in infrared spectroscopy shows a steep upturn at $\omega = 500 \sim 600 \text{ cm}^{-1}$ [6]. These experiments suggest the strong electron-boson coupling. Since the energy of these bosonic modes corresponds to the frequency of relevant optical phonons, EPI is expected to be strong in Na_xCoO_2 .

We have studied the electron-phonon mechanism for superconductivity in our previous paper [28], by noticing two kinds of the optical modes (breathing (A_{1g}) and shear (E_g) modes) that strongly couple with $3d$ electrons in Co. We have found that the shear mode phonon, which represents the oscillation of O ions parallel to the CoO_2 layer, induces the transition of Cooper pairs between different bands. Due to this mechanism, a considerably strong pairing interaction for s -wave pairing is realized, which is known as the Suhl-Kondo (SK) mechanism [29]. The SK mechanism works even if e'_g hole pockets are absent, as long as the top of the e'_g -band (valence band) is close to the Fermi level compared with phonon frequency [28]. In Ref. [28], we have discussed that s -wave superconductivity due to this "valence band SK effect" is expected to be realized in water-intercalated $\text{Na}_x\text{CoO}_2 \cdot y\text{H}_2\text{O}$ since the top of the valence band is supposed to approach the Fermi level [30, 31]. We note that extended s -wave scenario had been proposed based on the two concentric a_{1g} FSs model [32, 33].

However, we did not take account of the large Coulomb repulsive interaction in $3d$ orbitals of Co in Ref. [28], which works to prevent the s -wave pairing. It is an important problem to elucidate whether or not the attractive force due to EPI overcomes the Coulomb repulsion and an s -wave superconductivity can be realized. For that purpose, we have to know the values of EPI and the Coulomb interaction precisely. According to a recent first-principle cluster calculation based on a quantum chemical ab-initio method, the Coulomb interaction at Co site in Na_xCoO_2 is $4 \sim 5 \text{ eV}$ [34]. Also, the mass enhancement factor in M_xCoO_2 ($\text{M}=\text{Na}, \text{K}$ or Rb) due to optical phonons at $\sim 0.1 \text{ eV}$ is estimated to be $m^*/m \sim 2$ by ARPES measurement [16]. However, there is little information about the precise matrix elements of EPI in Na_xCoO_2 .

In this paper, we quantitatively examine the EPI between $3d$ electrons and relevant optical phonons that involve the deformation of CoO_6 octahedron. The EPI originates from both the change of the Coulomb potential and that of the transfer integral due to the displacement of O ions. We calculate the value of EPI using the second order perturbation of the transfer integral. We find that the EPI for shear phonon is considerably increased by the trigonal distortion of CoO_2 layer, which had not been taken into account in our previous study [28]. Thus, s -wave superconductivity can be realized in $\text{Na}_x\text{CoO}_2 \cdot y\text{H}_2\text{O}$ irrespective of the large Coulomb interaction $U \sim 5 \text{ eV}$. We also study the oxygen isotope effect on T_c , and find that it becomes very small when $U = 4 \sim 6 \text{ eV}$.

This paper is organized as follows. In §II, we derive the EPI microscopically in case with and without distortion of CoO_2 layers. We discuss the change of EPI due to intercalation of water. The erroneous result of EPI given in Ref. [28] is corrected. In §III, we explain the 3-band model for t_{2g} electron system, and we derive the linearized gap equation. In §IV, numerical results of the transition temperature are obtained by solving the gap equation numerically. In §V, we discuss the robustness of s -wave superconductivity over the strong Coulomb interaction. We also discuss the oxygen isotope effect and the possible mechanism of anisotropic s -wave superconducting state in $\text{Na}_x\text{CoO}_2 \cdot y\text{H}_2\text{O}$. Finally, results of this paper are summarized in §VI.

II. ELECTRON PHONON INTERACTION IN $\text{Na}_x\text{CoO}_2 \cdot y\text{H}_2\text{O}$

In this section, we derive the EPI in $\text{Na}_x\text{CoO}_2 \cdot y\text{H}_2\text{O}$ microscopically. This compound consists of two dimensional CoO_2 layers separated by a thick insulating layer composed of Na ions and H_2O molecules. CoO_2 layer comprises a triangular network of CoO_6 octahedra that share edges as shown in Fig. 1 (a). In this network, Co ions (black circles in Fig. 1 (a)) and O ions in the upper-layer (white circles) and lowerlayer (gray circles) forms

triangular lattices, respectively. Due to the crystalline electric field by octahedral coordination of O ion, five-fold $3d$ orbitals of Co ion split into threefold t_{2g} (d_{xy} , d_{yz} and d_{zx}) orbitals and twofold e_g ($d_{x^2-y^2}$ and $d_{3z^2-r^2}$) orbitals. Hereafter, we neglect e_g -orbitals since they are completely empty. In Na_xCoO_2 , CoO_6 octahedra are trigonally distorted along c -axis, so that CoO_2 layers become thinner. Due to this trigonal distortion, threefold t_{2g} orbitals split into the a_{1g} orbitals and twofold e'_g orbitals as shown in Fig. 2. According to the LDA calculations, the a_{1g} orbital forms large hole-like FS around the Γ -point and the e'_g orbitals form six hole pockets near the K-points. Since Na ions and O ions are monovalent cation and divalent anion, respectively, valence of Co ions is $\text{Co}^{(4-x)+}$ (mixed valence of Co^{3+} and Co^{4+}). Therefore, the number of $3d$ electron is $5+x$, that is, the number of hole in t_{2g} orbitals is $1-x$ in $\text{Na}_x\text{CoO}_2 \cdot y\text{H}_2\text{O}$. If the concentration of oxonium ion (H_3O^+) is z , the hole number is given by $1-x-z$ [35]. Since the present paper is devoted to the s -wave superconductivity due to the EPI, obtained results depends not on the hole number, but on the top of the e'_g -bands measured from the Fermi level. For this reason, we do not consider the existence of the oxonium ion hereafter.

Next, we determine the optical phonon modes that cause strong EPI. In Na_xCoO_2 , there are 14 kinds of optical modes at zone center [36]. Since the potentials of t_{2g} orbitals are considerably changed by the deformation of CoO_6 octahedron and each CoO_2 layer is almost isolated, we have only to consider single CoO_2 -layer phonon modes. According to Ref. [28], there are 4 single-layer phonon modes. Among them, the ungerade modes in which all O ions move in the same directions has no couplings with t_{2g} electrons within the linear term of the displacement. As a result, only the A_{1g} mode (breathing mode) and the E_{1g} mode (shear mode) strongly couple with t_{2g} electrons. In breathing mode and shear mode, O ions oscillate in the direction parallel and perpendicular to the CoO_2 layer, respectively, as shown in Fig. 1 (b).

Here, we describe the method of calculation of the EPI. We focus on the zone center modes and calculate the EPI via the frozen phonon method. To obtain the EPI, we calculate the change of potentials of t_{2g} orbitals due to the displacement of six O ions in CoO_6 octahedron, which is shown in Fig. 1 (c). We consider two types of contributions to the EPI; one is the Coulomb potential by O^{2-} ions, and the other is the effective potential due to the transfer integrals between Co and O. In Ref. [28], we consider the EPI due to transfer integrals up to the fourth order processes. However, the third order term was wrong in sign. After correcting this mistake, we verified that a reliable EPI can be obtained by the second order perturbation since the third order term and the fourth order term almost cancel. In the present study, we find that the effect of trigonal distortion on EPI, which was not taken into account in the previous study [28], is significant. The calculation of the EPI (in the presence of trigonal distortion) will be shown in §II A (§II B) in

detail.

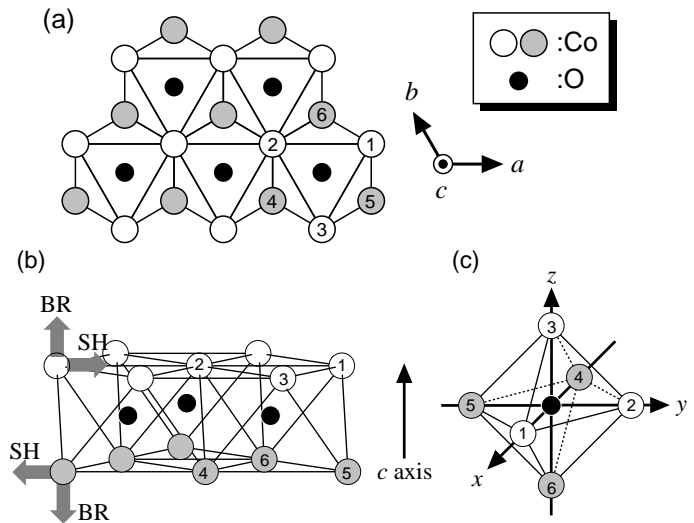


FIG. 1: (a), (b) Crystal structure of a CoO_2 layer. Co and O in upside ($\text{O}_1, \text{O}_2, \text{O}_3$) and downside ($\text{O}_4, \text{O}_5, \text{O}_6$) of CoO_2 layer forms triangular lattice, respectively. (c) The structure of CoO_6 octahedron without trigonal deformation. Note that z -axis does not correspond to c -axis.

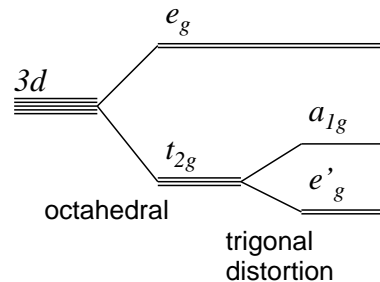


FIG. 2: Crystalline electronic field for d -electron in Na_xCoO_2 . The splitting between a_{1g} and e'_g is caused by the trigonal deformation of CoO_6 octahedron.

A. EPI in the absence of trigonal distortion

Here, we calculate the EPI between t_{2g} electrons and optical phonons in the absence of trigonal distortion of CoO_6 octahedron. We set the xyz coordinate system as shown in Fig. 1 (c). c and a crystal axes are along the $(1,1,1)$ and $(1,-1,0)$ directions in the xyz coordinate system, respectively. The coordinates of six O ions are $(\pm a, 0, 0)$, $(0, \pm a, 0)$, $(0, 0, \pm a)$, where positive (negative) sign corresponds to O_1, O_2 and O_3 (O_4, O_5 and O_6) ions that locate upper (lower) side of CoO_2 layer. In breathing and shear modes, O ions oscillate in the direction parallel and perpendicular to the c crystal axis, respectively. The displacement due to a breathing phonon is

$\mathbf{u}^{\text{BR}} = \pm \frac{u^{\text{BR}}}{\sqrt{3}}(1, 1, 1)$, where positive (negative) sign corresponds to the displacements of O_1 , O_2 and O_3 (O_4 , O_5 and O_6) ions. The displacement due to shear phonon is expressed as $\mathbf{u}^{\text{SH}} = \pm(v_1, v_2, -v_1 - v_2)$. Here, we choose the orthogonal bases as $\mathbf{u}^{\text{SH1}} = \pm \frac{u^{\text{SH1}}}{\sqrt{2}}(1, -1, 0)$ and $\mathbf{u}^{\text{SH2}} = \pm \frac{u^{\text{SH2}}}{\sqrt{6}}(1, 1, -2)$, where positive (negative) sign corresponds to the displacements of O_1 , O_2 and O_3 (O_4 , O_5 and O_6) ions.

Here, we calculate the EPI originates from the

$$\delta V_{\text{C}}^{\text{BR}}(\mathbf{r}) = \frac{2e^2}{4\pi\epsilon_0} \left(-\frac{2\sqrt{3}}{a^2} + \frac{4\sqrt{3}}{a^4}(xy + yz + zx) \right) u^{\text{BR}}, \quad (1)$$

$$\delta V_{\text{C}}^{\text{SH1}}(\mathbf{r}) = \frac{2e^2}{4\pi\epsilon_0} \left(-\frac{9\sqrt{2}}{2a^4}(x^2 - y^2) - \frac{3\sqrt{2}}{a^4}(yz - zx) \right) u^{\text{SH1}}, \quad (2)$$

$$\delta V_{\text{C}}^{\text{SH2}}(\mathbf{r}) = \frac{2e^2}{4\pi\epsilon_0} \left(-\frac{3\sqrt{6}}{2a^4}(x^2 + y^2 - 2z^2) + \frac{\sqrt{6}}{a^4}(2xy - yz - zx) \right) u^{\text{SH2}}, \quad (3)$$

where we have dropped the fourth and higher order terms in x , y and z . The matrix elements of the EPI due to Coulomb potential is given by $\langle \mu | \delta V_{\text{C}}^{\alpha} | \nu \rangle$, where $\mu, \nu = x, y, z$. Since the wave function for $\mu\nu$ -orbital ($\mu\nu = xy, yz$, or zx) is expressed as $\phi_{\mu\nu}(\mathbf{r}) = \sqrt{15} \frac{\mu\nu}{r^2} \phi(r)$, it is easy to show that $\langle yz | xy | zx \rangle = \frac{1}{7} \langle r^2 \rangle$, where $\langle r^2 \rangle =$

Coulomb potentials by using the point charge model. The Coulomb potentials $V_{\text{C}}(\mathbf{r})$ of an electron with charge $-e$ at the center of six O^{2-} ions is expressed as $V_{\text{C}}(\mathbf{r}) = \sum_{i=1,6} \frac{2e^2}{4\pi\epsilon_0} \frac{1}{|\mathbf{r}-\mathbf{r}_i|}$, where \mathbf{r}_i ($i = 1-6$) are the position vectors of O ions. Owing to the displacement of O ions due to α -mode phonon, $V_{\text{C}}(\mathbf{r})$ changes to $V_{\text{C}}^{\alpha}(\mathbf{r}) = \sum_{i=1,6} \frac{2e^2}{4\pi\epsilon_0} \frac{1}{|\mathbf{r}-\mathbf{r}_i-\mathbf{u}_i^{\alpha}|}$. To calculate the EPI, we expand $\delta V_{\text{C}}^{\alpha}(\mathbf{r}) \equiv V_{\text{C}}^{\alpha}(\mathbf{r}) - V_{\text{C}}(\mathbf{r})$ up to the first order in u^{α} as follows:

$\int \phi^2(r) d^3r$ is the expectation value of the square of the radius in $3d$ -orbital. We use the notation $r_d^2 = \langle r^2 \rangle$ hereafter. Similarly, $\langle zx | yz | xy \rangle = \langle xy | zx | yz \rangle = \frac{1}{7} r_d^2$. Thus, we obtain the EPI for breathing phonon as

$$\delta \hat{V}_{\text{C}}^{\text{BR}} = \frac{2e^2}{4\pi\epsilon_0} \left\{ -\frac{2\sqrt{3}}{a^2} \begin{bmatrix} 1 & 0 & 0 \\ 0 & 1 & 0 \\ 0 & 0 & 1 \end{bmatrix} + \frac{4\sqrt{3}r_d^2}{a^4} \begin{bmatrix} 0 & \frac{1}{7} & \frac{1}{7} \\ \frac{1}{7} & 0 & \frac{1}{7} \\ \frac{1}{7} & \frac{1}{7} & 0 \end{bmatrix} \right\} u^{\text{BR}},$$

where the first, the second and the third column (row) correspond to d_{xy} , d_{yz} and d_{zx} orbitals, respectively.

Here, we change the basis of t_{2g} -orbitals from the (d_{xy}, d_{yz}, d_{zx}) -basis into the (a_{1g}, e_g^1, e_g^2) -basis, which is the basis of the irreducible representation under the trigonal crystalline electric field. The transformation matrix \hat{U} from the (d_{xy}, d_{yz}, d_{zx}) -basis to the (a_{1g}, e_g^1, e_g^2) -basis is given by

$$\begin{aligned} \begin{pmatrix} |a_{1g}\rangle \\ |e_g^1\rangle \\ |e_g^2\rangle \end{pmatrix} &= \hat{U} \begin{pmatrix} |xy\rangle \\ |yz\rangle \\ |zx\rangle \end{pmatrix} \\ &= \begin{pmatrix} \frac{1}{\sqrt{3}} & \frac{1}{\sqrt{3}} & \frac{1}{\sqrt{3}} \\ 0 & \frac{1}{\sqrt{2}} & -\frac{1}{\sqrt{2}} \\ \frac{2}{\sqrt{6}} & -\frac{1}{\sqrt{6}} & -\frac{1}{\sqrt{6}} \end{pmatrix} \begin{pmatrix} |xy\rangle \\ |yz\rangle \\ |zx\rangle \end{pmatrix}. \quad (4) \end{aligned}$$

By operating \hat{U} and \hat{U}^{\dagger} on the left side and the right side of the matrix in Eq. (4), respectively, the matrix form of the EPI in the (a_{1g}, e_g^1, e_g^2) -basis is given by

$$\delta \hat{V}_{\text{C}}^{\text{BR}} = \begin{pmatrix} a_1^{\text{C}} & 0 & 0 \\ 0 & a_2^{\text{C}} & 0 \\ 0 & 0 & a_2^{\text{C}} \end{pmatrix} \tilde{u}^{\text{BR}}, \quad (5)$$

$$a_1^{\text{C}} = -\frac{2e^2}{4\pi\epsilon_0} \cdot \frac{2\sqrt{3}}{a^2} \sqrt{\frac{\hbar}{2M\omega_{\text{BR}}}} \left(1 - \frac{4r_d^2}{7a^2} \right), \quad (6)$$

$$a_2^{\text{C}} = -\frac{2e^2}{4\pi\epsilon_0} \cdot \frac{2\sqrt{3}}{a^2} \sqrt{\frac{\hbar}{2M\omega_{\text{BR}}}} \left(1 + \frac{2r_d^2}{7a^2} \right). \quad (7)$$

Here, we introduce a dimensionless parameter $\tilde{u}^{\alpha} = u^{\alpha} / \sqrt{\hbar/2M\omega_{\alpha}}$ that represents a displacement due to α -mode phonon as the unit of zero-point motion

$\sqrt{\hbar/2M\omega_\alpha}$, where ω_α is the frequency of α -mode phonon. Then, \hat{u}^α is expressed by the sum of creation and annihilation operators for the α -mode phonon, $\hat{u}^\alpha = b_\alpha + b_\alpha^\dagger$.

Next, we calculate the EPI for shear phonons. Using

$$\begin{aligned} \delta\hat{V}_C^{\text{SH1}} &= \frac{2e^2}{4\pi\epsilon_0} \left\{ -\frac{9\sqrt{2}r_d^2}{2a^4} \begin{bmatrix} 0 & 0 & 0 \\ 0 & -\frac{2}{7} & 0 \\ 0 & 0 & \frac{2}{7} \end{bmatrix} - \frac{3\sqrt{2}r_d^2}{a^4} \begin{bmatrix} 0 & -\frac{1}{7} & \frac{1}{7} \\ -\frac{1}{7} & 0 & 0 \\ \frac{1}{7} & 0 & 0 \end{bmatrix} \right\} u^{\text{SH1}} \\ &= \frac{2e^2}{4\pi\epsilon_0} \cdot \frac{3\sqrt{2}r_d^2}{7a^4} \begin{bmatrix} 0 & 1 & -1 \\ 1 & 3 & 0 \\ -1 & 0 & -3 \end{bmatrix} u^{\text{SH1}}, \end{aligned} \quad (8)$$

$$\begin{aligned} \delta\hat{V}_C^{\text{SH2}} &= \frac{2e^2}{4\pi\epsilon_0} \left\{ -\frac{3\sqrt{6}r_d^2}{2a^4} \begin{bmatrix} \frac{4}{7} & 0 & 0 \\ 0 & -\frac{2}{7} & 0 \\ 0 & 0 & -\frac{2}{7} \end{bmatrix} + \frac{\sqrt{6}r_d^2}{a^4} \begin{bmatrix} 0 & -\frac{1}{7} & -\frac{1}{7} \\ -\frac{1}{7} & 0 & \frac{2}{7} \\ -\frac{1}{7} & \frac{2}{7} & 0 \end{bmatrix} \right\} u^{\text{SH2}} \\ &= \frac{2e^2}{4\pi\epsilon_0} \cdot \frac{\sqrt{6}r_d^2}{7a^4} \begin{bmatrix} -6 & -1 & -1 \\ -1 & 3 & 2 \\ -1 & 2 & 3 \end{bmatrix} u^{\text{SH2}}, \end{aligned} \quad (9)$$

By transforming Eqs. (8)-(9) into the expression in the (a_{1g}, e_g^1, e_g^2) -basis, we obtain

$$\delta\hat{V}_C^{\text{SH1}} = \begin{pmatrix} 0 & b_1^C & 0 \\ b_1^C & 0 & -b_2^C \\ 0 & -b_2^C & 0 \end{pmatrix} \hat{u}^{\text{SH1}}, \quad (10)$$

$$\delta\hat{V}_C^{\text{SH2}} = \begin{pmatrix} 0 & 0 & -b_1^C \\ 0 & b_2^C & 0 \\ -b_1^C & 0 & -b_2^C \end{pmatrix} \hat{u}^{\text{SH2}}, \quad (11)$$

$$\begin{aligned} b_1^C &= \langle a_{1g} | \delta V_C^{\text{SH1}} | e_g^1 \rangle \\ &= \frac{2e^2}{4\pi\epsilon_0} \cdot \frac{2\sqrt{3}}{a^2} \sqrt{\frac{\hbar}{2M\omega_{\text{SH}}}} \frac{4r_d^2}{7a^2}, \end{aligned} \quad (12)$$

$$b_2^C = \langle e_g^1 | \delta V_C^{\text{SH2}} | e_g^1 \rangle = b_1^C / (4\sqrt{2}). \quad (13)$$

Thus, the EPI originating from the Coulomb potential is represented by four coupling constants a_1^C , a_2^C , b_1^C and b_2^C .

Next, we derive the EPI that originates from the changes of d - p transfer integrals between Co and O. For this purpose, we consider the CoO_6 octahedron in which Co^{4+} ion (hole number is unity) is surrounded by six O^{2-} (no holes) ions. In this octahedron, the uncertainty principle allows the virtual process in which a hole in d orbitals transfers to p orbitals and turns back. By this second-order process, the effective potential of a hole in d orbitals is lowered by $-t_{pd}^2/\Delta_{pd}$, where t_{pd} is the d - p transfer integral and $\Delta_{pd}(>0)$ is the charge transfer energy. When the transfer integral is changed by δt_{pd} , the

$\langle xy|x^2|xy \rangle = \langle zx|x^2|zx \rangle = \frac{3}{7}r_d^2$ and $\langle yz|x^2|yz \rangle = \frac{1}{7}r_d^2$, we obtain the matrix form of the EPI for shear phonons from Eqs. (2)-(3) in the (d_{xy}, d_{yz}, d_{zx}) -basis as

effective potential of a hole becomes $-(t_{pd} + \delta t_{pd})^2/\Delta_{pd}$. Thus, in the electron representation, the change of the effective potential is given by $\delta V_T = 2t_{pd}\delta t_{pd}/\Delta_{pd}$. In

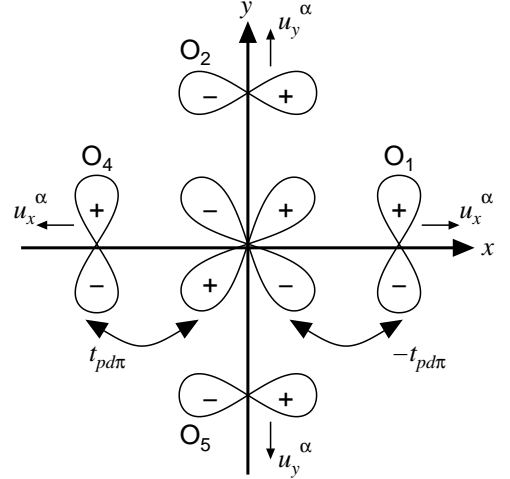


FIG. 3: Transfer integrals between d_{xy} orbital in Co and (p_x, p_y) orbitals in O. In this figure, d_{xy} electron can transfer to p_y orbitals in O_1 and O_4 via $\pm t_{pd\pi}$.

CoO_6 octahedron, the total change of the effective potential $(\delta V_T)_{ll'}$ for d -orbital is given by

$$(\delta V_{\text{T}}^{\alpha})_{ll'} = \sum_{i=1-6} \sum_{m=p_x, p_y, p_z} \frac{t_{pd}(i, l, m) \delta t_{pd}^{\alpha}(i, l', m) + t_{pd}(i, l', m) \delta t_{pd}^{\alpha}(i, l, m)}{\Delta_{pd}}, \quad (14)$$

where $t_{pd}(i, l, m)$ represents the d - p transfer integrals between l orbital of Co ($l = d_{xy}, d_{yz}, d_{zx}$) and m orbital of O ($m = p_x, p_y, p_z$) at i site ($i = 1 \sim 6$), and $\delta t_{pd}^{\alpha}(i, l, m)$ is the change of $t_{pd}(i, l, m)$ due to α -mode phonon. In the absence of trigonal distortion, $t_{pd}(i, l, m)$ is given by Slater-Koster parameter $t_{pd\pi}$ only, as shown in Fig. 3. For example, $t_{pd}(i = 1, l = d_{xy}, m = p_y) = -t_{pd\pi}$ and $t_{pd}(i = 4, l = d_{xy}, m = p_y) = t_{pd\pi}$. According to Harrison's law [37], $t_{pd\pi}$ is proportional to a^{-4} , where a is the distance between Co and O. Then, $\delta t_{pd\pi} = -t_{pd\pi} \frac{4}{a} \delta a$.

Now, we calculate $(\delta V_{\text{T}}^{\text{BR}})_{ll}$. Since $\delta a = u^{\text{BR}}/\sqrt{3}$ for breathing phonon, $\delta t_{pd}^{\text{BR}}(i, l, m) = -t_{pd}(i, l, m) \frac{4}{\sqrt{3}a} u^{\text{BR}}$. For each l , $t_{pd}(i, l, m)$ is finite only for four sets of (i, m) . After taking the summation of i and m in Eq. (14), we obtain $(\delta V_{\text{T}}^{\alpha})_{ll} = -8t_{pd\pi}^2 u^{\text{BR}}/(\sqrt{3}\Delta_{pd}a) \times 4 = -32t_{pd\pi}^2 u^{\text{BR}}/(\sqrt{3}\Delta_{pd}a)$. By performing similar analysis, we obtain $(\delta V_{\text{T}}^{\text{BR}})_{ll'} = 4t_{pd\pi}^2 u^{\text{BR}}/(\sqrt{3}\Delta_{pd}a)$ for $l \neq l'$ by using the Slater Koster formula [38], without necessity to use Harrison's law. As a result, the matrix representation for breathing phonon in the (d_{xy}, d_{yz}, d_{zx}) -basis is expressed as follows:

$$\delta \hat{V}_{\text{T}}^{\text{BR}} = \begin{bmatrix} 8 & -1 & -1 \\ -1 & 8 & -1 \\ -1 & -1 & 8 \end{bmatrix} \frac{4t_{pd\pi}^2}{\sqrt{3}\Delta_{pd}a} u^{\text{BR}}. \quad (15)$$

Equation (15) is transformed in the (a_{1g}, e_g^1, e_g^2) -basis as

$$\delta \hat{V}_{\text{T}}^{\text{BR}} = \begin{pmatrix} a_1^{\text{T}} & 0 & 0 \\ 0 & a_2^{\text{T}} & 0 \\ 0 & 0 & a_2^{\text{T}} \end{pmatrix} \tilde{u}^{\text{BR}}, \quad (16)$$

$$a_1^{\text{T}} = \frac{2}{3}a_2^{\text{T}} = -\frac{24}{\sqrt{3}} \cdot \frac{t_{pd\pi}^2}{\Delta_{pd}a} \sqrt{\frac{\hbar}{2M\omega_{\text{BR}}}}. \quad (17)$$

In the same way, we can derive the EPI for shear phonons. For SH1 mode ($\mathbf{u}_{\text{SH1}} = \pm \frac{u^{\text{SH1}}}{\sqrt{2}}(1, -1, 0)$), $\delta a = u/\sqrt{2}$ for O_1 and O_4 , $\delta a = -u/\sqrt{2}$ for O_2 and O_5 , and $\delta a = 0$ for O_3 and O_6 . Therefore, $\delta t_{pd}^{\text{SH1}}(i, l, m) = -t_{pd}(i, l, m) \frac{4}{\sqrt{2}a} u^{\text{SH1}}$ for $i = 1, 4$, $t_{pd}(i, l, m) \frac{4}{\sqrt{2}a} u^{\text{SH1}}$ for $i = 2, 5$, and 0 for $i = 3, 6$. For SH2 mode ($\mathbf{u}_{\text{SH2}} = \pm \frac{u^{\text{SH2}}}{\sqrt{6}}(1, 1, -2)$), $\delta t_{pd}^{\text{SH2}}(i, l, m) = -t_{pd}(i, l, m) \frac{4}{\sqrt{6}a} u^{\text{SH1}}$ for $i = 1, 2, 4, 5$, and $t_{pd}(i, l, m) \frac{8}{\sqrt{6}a} u^{\text{SH1}}$ for $i = 3, 6$. As a result, we obtain

$$\delta \hat{V}_{\text{T}}^{\text{SH1}} = \begin{bmatrix} 0 & 1 & -1 \\ 1 & 8 & 0 \\ -1 & 0 & -8 \end{bmatrix} \frac{\sqrt{2}t_{pd\pi}^2 u^{\text{SH}}}{\Delta_{pd}a} \quad (18)$$

$$\delta \hat{V}_{\text{T}}^{\text{SH2}} = \begin{bmatrix} -16 & -1 & -1 \\ -1 & 8 & 2 \\ -1 & 2 & 8 \end{bmatrix} \sqrt{\frac{2}{3}} \frac{t_{pd\pi}^2 u^{\text{SH}}}{\Delta_{pd}a} \quad (19)$$

By transforming Eqs. (18)-(19) into (a_{1g}, e_g^1, e_g^2) -basis, we obtain

$$\delta \hat{V}_{\text{T}}^{\text{SH1}} = \begin{pmatrix} 0 & b_1^{\text{T}} & 0 \\ b_1^{\text{T}} & 0 & -b_2^{\text{T}} \\ 0 & -b_2^{\text{T}} & 0 \end{pmatrix} \tilde{u}^{\text{SH1}}, \quad (20)$$

$$\delta \hat{V}_{\text{T}}^{\text{SH2}} = \begin{pmatrix} 0 & 0 & -b_1^{\text{T}} \\ 0 & b_2^{\text{T}} & 0 \\ -b_1^{\text{T}} & 0 & -b_2^{\text{T}} \end{pmatrix} \tilde{u}^{\text{SH2}}, \quad (21)$$

$$b_1^{\text{T}} = \frac{3}{\sqrt{2}}b_2^{\text{T}} = 6\sqrt{3} \cdot \frac{t_{pd\pi}^2}{\Delta_{pd}a} \sqrt{\frac{\hbar}{2M\omega_{\text{SH}}}}. \quad (22)$$

Thus, the EPI originating from d - p transfer integrals is represented by four coupling constants a_1^{T} , a_2^{T} , b_1^{T} and b_2^{T} .

B. EPI in the presence of trigonal distortion

In §II A, we have calculated the EPI in the absence of trigonal distortion. However, CoO_2 layer in Na_xCoO_2 becomes thinner due to the trigonal distortion, and it is increased by the water intercalation. Since this change of crystal structure can modify the EPI prominently, we calculate the EPI in the presence of trigonal distortion in this subsection.

Owing to the trigonal distortion, the position of O ions move along the c crystal axis. Then, the changes of the coordinates of O_1 , O_2 and O_3 are $(-b/\sqrt{3}, -b/\sqrt{3}, -b/\sqrt{3})$ and that for O_4 , O_5 and O_6 are $(b/\sqrt{3}, b/\sqrt{3}, b/\sqrt{3})$, where $b (> 0)$ is the magnitude of displacement. According to the neutron scattering measurement [39], O_1 -Co- O_5 angle θ_{15} for unhydrated Na_xCoO_2 and hydrated $\text{Na}_x\text{CoO}_2 \cdot y\text{H}_2\text{O}$ are 84° and 82° , respectively. Thus, we can determine the value of b from θ_{15} by solving the following equation.

$$\cos \theta_{15} = -(3m^2 - 2m)/(3m^2 - 2m + 1), \quad (23)$$

where $m = b/(\sqrt{3}a)$. Using the values of b obtained in Eq. (23), we derive the EPI in the presence of trigonal distortion as follows.

First, we calculate the EPI originating from the change of the Coulomb potential. In the case of $m = 0$, the u^{α} -linear terms of the Coulomb potentials are given in Eqs. (1)-(3). Up to the first order of $m = b/(\sqrt{3}a)$, they are modified as

$$\delta V_C^{\text{BR}}(\mathbf{r}) = \frac{2e^2}{4\pi\epsilon_0} \left(-\frac{2\sqrt{3}}{a^2} + \frac{4\sqrt{3}}{a^4}(1+7m)(xy+yz+zx) \right) u^{\text{BR}}, \quad (24)$$

$$\delta V_C^{\text{SH1}}(\mathbf{r}) = \frac{2e^2}{4\pi\epsilon_0} \left(-\frac{9\sqrt{2}}{2a^4}(x^2-y^2) - \frac{3\sqrt{2}}{a^4}(yz-zx) \right) (1+7m)u^{\text{SH1}}, \quad (25)$$

$$\delta V_C^{\text{SH2}}(\mathbf{r}) = \frac{2e^2}{4\pi\epsilon_0} \left(-\frac{3\sqrt{6}}{2a^4}(x^2+y^2-2z^2) + \frac{\sqrt{6}}{a^4}(2xy-yz-zx) \right) (1+7m)u^{\text{SH2}}. \quad (26)$$

As a result, the coupling constants a_1^C , a_2^C , b_1^C and b_2^C are given by

$$a_1^C = \frac{2e^2}{4\pi\epsilon_0} \cdot \frac{2\sqrt{3}}{a^2} \sqrt{\frac{\hbar}{2M\omega_{\text{BR}}}} \left(1 - \frac{4r_d^2}{7a^2}(1+7m) \right), \quad (27)$$

$$a_2^C = \frac{2e^2}{4\pi\epsilon_0} \cdot \frac{2\sqrt{3}}{a^2} \sqrt{\frac{\hbar}{2M\omega_{\text{BR}}}} \left(1 + \frac{2r_d^2}{7a^2}(1+7m) \right), \quad (28)$$

$$b_1^C = 4\sqrt{2}b_2^C = \frac{2e^2}{4\pi\epsilon_0} \cdot \frac{2\sqrt{3}}{a^2} \sqrt{\frac{\hbar}{2M\omega_{\text{SH}}}} \frac{4r_d^2}{7a^2}(1+7m). \quad (29)$$

The values of m at $\theta_{15} = 84^\circ$ and 82° are $m \simeq 0.051$ and 0.068 , respectively. Therefore, b_1^C and b_2^C at $\theta_{15} = 84^\circ$ and 82° are about 40 % larger than the values at $\theta_{15} = 90^\circ$. The estimated values of a_1^C , a_2^C , b_1^C and b_2^C are shown in Table I. In calculating these values, we use $\frac{2e^2}{4\pi\epsilon_0 a} = 14.4$ eV ($a = 2.0$ Å), $M = 26.561 \times 10^{-27}$ kg (the mass of ^{16}O ion), $r_d = 0.6$ Å (radius of Co ion [40]), $\omega_{\text{BR}} = 580$ cm $^{-1}$ and $\omega_{\text{SH}} = 480$ cm $^{-1}$ [41]. In Eqs. (24)-(29), we show the results up to the first order of m . In calculating the values of a_1 , a_2 , b_1 and b_2 in Table I, we use the exact expressions for them with respect to m .

Next, we calculate the EPI due to the change of d - p transfer integrals. In the absence of trigonal distortion, we have only to consider the contribution of $t_{pd\pi}$ to $t_{pd}(i, l, m)$. In contrast, we have also to consider the contribution of $t_{pd\sigma}$ in the presence of trigonal distortion, and the d - p transfer integral $t_{pd}(i, l, m)$ is given by using the Slater-Koster formula [38]. Then, we can obtain $\delta t_{pd}^\alpha(i, l, m)$ with the aid of the Harrison's law $t \propto a^{-4}$ [37]. As a result, EPI can be derived from Eq. (14). The obtained values of a_1^T , a_2^T , b_1^T and b_2^T are shown in Table I. In calculating these values, we use $t_{pd\sigma} = -1.70$ eV, $t_{pd\pi} = 0.785$ eV and $\Delta_{pd} = 1.81$ eV according to Ref. [19].

We have calculated the EPI between t_{2g} electrons and zone center phonons ($\mathbf{q}=0$). Hereafter, we neglect the \mathbf{q} -dependences of the EPI matrix elements for simplicity, by expecting that their \mathbf{q} -dependences are smeared out after the \mathbf{q} -summation. The dimensionless displacement due to α -mode phonon in EPI can be expressed as the sum of creation and annihilation operators for phonon, $\tilde{u}_{\mathbf{q}}^\alpha = b_{\alpha, \mathbf{q}} + b_{\alpha, \mathbf{q}}^\dagger$. Then, the Hamiltonian of EPI between t_{2g}

θ_{15}	90°	84°	82°	θ_{15}	90°	84°	82°
a_1^C	-1.01	-0.96	-0.94	a_1^T	-0.0675	-0.121	-0.147
a_2^C	-1.09	-1.08	-1.07	a_2^T	-0.101	-0.162	-0.189
b_1^C	0.0621	0.0874	0.0971	b_1^T	0.0557	0.108	0.136
b_2^C	0.0110	0.0142	0.0146	b_2^T	0.0262	0.0524	0.0629

TABLE I: Obtained electron-phonon coupling constants originating from the change of the Coulomb potential (left panel) and the change of d - p transfer integrals (right panel) for $\theta_{15} = 90^\circ, 84^\circ$ and 82°

θ_{15}	90°	84°	82°
a_1	-0.215	-0.218	-0.218
a_2	-0.239	-0.249	-0.252
b_1	0.118	0.196	0.233
b_2	0.0372	0.0665	0.0775

TABLE II: Total electron-phonon coupling constants for $\theta_{15} = 90^\circ, 84^\circ$ and 82°

electrons and optical phonons are represented as follows.

$$H_{\text{EPI}} = \frac{1}{\sqrt{N}} \sum_{\alpha} \sum_{\mathbf{k}, \mathbf{q}, \sigma} \hat{c}_{\mathbf{k}+\mathbf{q}\sigma}^\dagger \hat{V}^\alpha \hat{c}_{\mathbf{k}\sigma} (b_{\alpha, \mathbf{q}} + b_{\alpha, -\mathbf{q}}^\dagger) \quad (30)$$

where $\hat{c}_{\mathbf{k}\sigma} = (c_{\mathbf{k}, a_{1g}, \sigma} \ c_{\mathbf{k}, e_g^1, \sigma} \ c_{\mathbf{k}, e_g^2, \sigma})$ is the column vector of annihilation operators for electrons, and $b_{\alpha, \mathbf{q}}$ is annihilation operator of α -mode phonon. Then, \hat{V}^α has

the following form:

$$\hat{V}^{\text{BR}} = \begin{pmatrix} a_1 & 0 & 0 \\ 0 & a_2 & 0 \\ 0 & 0 & a_2 \end{pmatrix}, \quad (31)$$

$$\hat{V}^{\text{SH1}} = \begin{pmatrix} 0 & b_1 & 0 \\ b_1 & 0 & -b_2 \\ 0 & -b_2 & 0 \end{pmatrix}, \quad \hat{V}^{\text{SH2}} = \begin{pmatrix} 0 & 0 & -b_1 \\ 0 & b_2 & 0 \\ -b_1 & 0 & -b_2 \end{pmatrix}. \quad (32)$$

where $a_i = a_i^C + a_i^T$ and $b_i = b_i^C + b_i^T$ ($i = 1, 2$). The estimated values of these coupling constants are shown in Table II. In estimating a_1 and a_2 , we have considered the screening effect by taking account of the chemical potential shift $\delta\mu$: To conserve the electron number, $\delta\mu$ should satisfy the relation $\rho_d(0)(\delta\varepsilon_d + \delta\mu) + \rho_p(0)\delta\mu = 0$, where $\rho_d(0)$ and $\rho_p(0)$ are the DOS of d -electrons and p -electrons at the Fermi level [28]. Then, the shift in the $3d$ level is $\delta\tilde{\varepsilon}_d \equiv \delta\varepsilon_d + \delta\mu = \rho_p(0)/[\rho_d(0) + \rho_p(0)]\delta\varepsilon_d$. Since $\rho_p(0)/[\rho_d(0) + \rho_p(0)] \approx 0.2$ in Na_xCoO_2 [14, 19], both a_1 and a_2 are reduced to 20% of their original (unscreened) values. On the other hand, such a screening effect is absent for shear phonons since $\text{Tr}\{\hat{V}^{\text{SH}}\}$ is equal to 0. In later sections, we use $b_1 = 0.20$ and $b_2 = 0.067$ (eV) for the unhydrated Na_xCoO_2 ($\theta_{15} = 84^\circ$), and $b_1 = 0.23$ and $b_2 = 0.078$ (eV) for the hydrated Na_xCoO_2 ($\theta_{15} = 82^\circ$). In both cases, we set $a_1 = 0.22$ and $a_2 = 0.25$ (eV).

III. DERIVATION OF GAP EQUATION

In this section, we formulate the model and derive the linearized gap equation. First, we explain the energy dependence of the DOS in the present model. In Na_xCoO_2 , there are three electronic bands (one a_{1g} -band and two e'_g -bands) near the Fermi level, which are composed of $3d$ orbitals of Co ion and $2p$ orbitals of O ion in CoO_2 layer. In these bands, the a_{1g} -band crosses the Fermi level, and the e'_g -bands are below the Fermi level (valence bands). Figure 4 shows the d -electron DOS of each band per spin that is obtained by the tight-binding model given in Ref. [19]. In the numerical study, we approximate d -electron DOS by the following rectangle function.

$$\rho_{a_{1g}}(\omega) = \begin{cases} 1.38 & (-0.92 \leq \omega \leq -0.73) \\ 0.38 & (-0.73 \leq \omega \leq 0.3) \\ 3.65 & (0.3 \leq \omega \leq 0.34) \end{cases}, \quad (33)$$

$$\rho_{e'_g}(\omega) = \begin{cases} 0.15 & (\Delta - 1.25 \leq \omega \leq \Delta - 0.85) \\ 1.75 & (\Delta - 0.85 \leq \omega \leq \Delta - 0.65) \\ 0.6 & (\Delta - 0.65 \leq \omega \leq \Delta) \end{cases} \quad (34)$$

where Δ (< 0) is the top of the e'_g bands measured from the Fermi level. The total d -electron DOS is $\rho_{a_{1g}}(\omega) + 2\rho_{e'_g}(\omega)$. Here, we regard Δ as variable. Equations (33) and (34) are shown in Fig. 4 (a) and (b), respectively.

Both $\rho_{a_{1g}}(\omega)$ and $\rho_{e'_g}(\omega)$ in Eqs. (33) and (34) are equal to the values in the tight binding model at $\omega = 0$ and $\omega = \Delta$. Note that $\int_{-\infty}^{\infty} \rho_{a_{1g}}(\omega)d\omega = \int_{-\infty}^{\infty} \rho_{e'_g}(\omega)d\omega = 0.8$ in accord with the band calculation [14] as well as the tight binding model [19]. Here, the number of hole is 0.65, which corresponds the hole number of $\text{Na}_{0.35}\text{CoO}_2$.

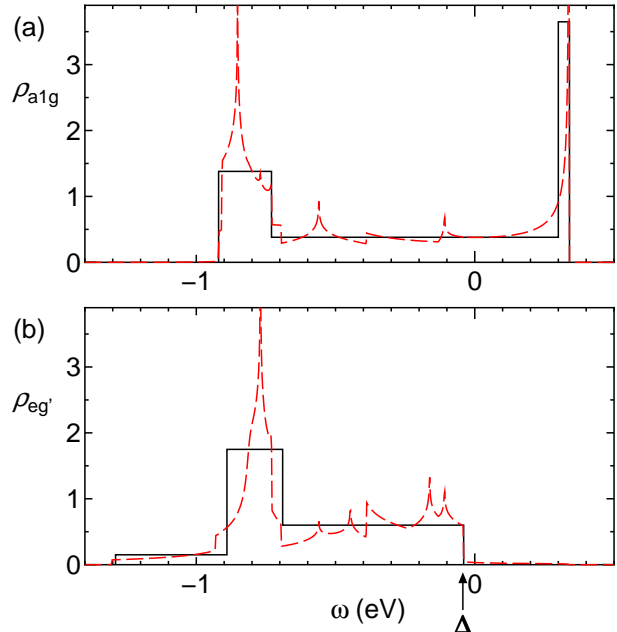


FIG. 4: (Color online) d -electron DOS for the a_{1g} -band and the e'_g -band per orbit and spin. Solid line represents the DOS used in the present study (solid line), and dashed line represents the DOS given by the tight-binding model. Note that $\rho_{e'_g}(\omega)$ in the tight-binding model takes small values for $\omega > \Delta$, since the a_{1g} -band that forms the large FS around Γ point contains small amount of e'_g -orbitals.

Although LDA band calculation predicts $\Delta > 0$ (i.e., presence of e'_g hole pockets) [14], the relation $\Delta < 0$ had been confirmed experimentally [15, 17, 18]. To solve this discrepancy, many people had studied the strong correlation effect, which is neglected in the LDA, using the Gutzwiller approximation [42] and the dynamical mean field approximation [43, 44]. References [42, 44] claim that e'_g hole pockets predicted by the LDA disappears (i.e., $\Delta < 0$) due to strong Coulomb interaction. We had also pointed out in Ref. [28] that the EPI (due to shear phonon) shifts the e'_g -bands downwards by -0.05 eV. In the present paper, we treat Δ as a model parameter.

A. gap equation

In Ref. [28], we have studied the linearized gap equation for s -wave superconductivity in the 11-band d - p model. The obtained gap function $\phi_U(i\varepsilon_n)$ does not have

the off-diagonal components ($l \neq l'$) where l, l' are the indexes of orbital ($l, l' = a_{1g}, e_g^1, e_g^2$). Moreover, gap functions for e_g^1 and e_g^2 are the same. Then, the linearized gap equation given by Eq. (8) in Ref. [28], which is 3×3 matrix equation, can be reduced to the following 1×2 matrix equation:

$$\lambda \hat{\phi}(i\varepsilon_n) = T \sum_m \hat{V}_{\text{eff}}(i\omega_m) \hat{F}(i\varepsilon_n - i\omega_m), \quad (35)$$

$$\begin{aligned} F_l(i\varepsilon_n) &= \frac{1}{N} \sum_{\mathbf{k}, l'} |G_{ll'}(\mathbf{k}, i\varepsilon_n)|^2 \phi_l'(i\varepsilon_n) \\ &\cong \phi_l(i\varepsilon_n) \frac{1}{N} \sum_{\mathbf{k}} |G_{ll}(\mathbf{k}, i\varepsilon_n)|^2, \end{aligned} \quad (36)$$

where $\hat{\phi}(i\varepsilon_n) = (\phi_{a_{1g}}(i\varepsilon_n), \phi_{e_g'}(i\varepsilon_n))$ and $\hat{F}(i\varepsilon_n) = (F_{a_{1g}}(i\varepsilon_n), F_{e_g'}(i\varepsilon_n))$ are column vectors of the gap functions and the linearized anomalous Green functions, respectively, and $G_{ll'}(\mathbf{k}, i\varepsilon_n)$ is the normal Green function. $\varepsilon_n = (2n+1)\pi T$ and $\omega_m = 2m\pi T$ are the Matsubara frequencies for fermion and boson, respectively. In Eq. (36), the eigenvalue of the gap equation, λ , increases monotonically as the temperature decreases, and T_c is determined by the condition $\lambda = 1$. In Eq. (36), we ignore the contribution of $l \neq l'$ since the off-diagonal components of Green function are small. Then, the diagonal component of Green function is approximately given by $G_{ll}(\mathbf{k}, i\varepsilon_n) = (i\varepsilon_n - E_{\mathbf{k}}^l - \Sigma^l(\mathbf{k}, i\varepsilon_n))^{-1}$, where $\Sigma^l(\mathbf{k}, i\varepsilon_n)$ is the d -electron self-energy. For the effective interaction of Cooper pairs $\hat{V}_{\text{eff}}(i\omega_m)$, we consider the EPI given by Eq. (30) and the Coulomb interaction $H_U + H_J$, where

$$H_U = \frac{U}{N} \sum_{\mathbf{k}, \mathbf{k}', \mathbf{q}} \sum_l c_{\mathbf{k}, l, \uparrow}^\dagger c_{\mathbf{k}', l, \downarrow}^\dagger c_{\mathbf{k}' - \mathbf{q}, l, \downarrow} c_{\mathbf{k} + \mathbf{q}, l, \uparrow} \quad (37)$$

$$H_J = \frac{J}{N} \sum_{\mathbf{k}, \mathbf{k}', \mathbf{q}} \sum_{l, l' \neq l} c_{\mathbf{k}, l, \uparrow}^\dagger c_{\mathbf{k}', l, \downarrow}^\dagger c_{\mathbf{k}' - \mathbf{q}, l', \downarrow} c_{\mathbf{k} + \mathbf{q}, l', \uparrow} \quad (38)$$

where U and J are the on-site Coulomb interaction in the same orbital and the pair hopping potential between different orbits, respectively. Hereafter, we set $J = U/10$ according to the first principle calculation in Ref. [19].

Since we have assumed that p -electrons are noninteracting, $\hat{V}_{\text{eff}}(i\omega_m)$ works only for d -electrons. Note that we do not have to consider the Coulomb interaction between different orbitals (U') and the Hund's coupling term (J_H) since the off-diagonal components of gap function are absent. Now, we treat H_U and H_J in the Hartree-Fock approximation, by extending the theory of Morel and Anderson [45]. Then, $\hat{V}_{\text{eff}}(i\omega_m)$ is given by

$$\begin{aligned} \hat{V}_{\text{eff}}(i\omega_m) &= \begin{pmatrix} a_1^2 & 0 \\ 0 & a_2^2 \end{pmatrix} D_{\text{BR}}(i\omega_m) + \begin{pmatrix} 0 & 2b_1^2 \\ b_1^2 & 2b_2^2 \end{pmatrix} D_{\text{SH}}(i\omega_m) \\ &\quad - \begin{pmatrix} U & 2J \\ J & U + J \end{pmatrix}, \end{aligned} \quad (39)$$

where $D_\alpha(i\omega_m) = 2\omega_\alpha/(\omega_\alpha^2 + \omega_m^2)$ is the phonon Green function for α -mode. ω_α is the Debye frequency of α -mode phonon. The first two terms in Eq. (39) represent attractive forces due to EPI, and the last term represents the repulsive force due to the Coulomb interaction. We see that attractive force induced by breathing phonon, which corresponds to the first term in Eq. (39), is reduced by U (or $U + J$). On the other hand, attractive force due to shear phonon is reduced by J (or $2J$).

Here, we calculate $F_l(i\varepsilon_n)$ in Eq. (36). Instead of summing \mathbf{k} in the right-hand side, we perform the energy integration as

$$\frac{1}{N} \sum_{\mathbf{k}} |G_{ll}(\mathbf{k}, i\varepsilon_n)|^2 = \int_{-\infty}^{\infty} \frac{z_l(\omega) \rho_l(\omega)}{\omega^2 + \varepsilon_n^2} d\omega, \quad (40)$$

where $\rho_l(\omega)$ is the d -electron DOS defined in Eqs. (33)-(34), and $z_l(\omega)$ is the renormalization factor given by the self-energy. The renormalization factor due to EPI at $\omega = 0$ is given by $z_l(0) = \left(1 - \frac{\partial \Sigma_l^{\text{BR}}(\omega)}{\partial \omega} \Big|_{\omega=0} - \frac{\partial \Sigma_l^{\text{SH}}(\omega)}{\partial \omega} \Big|_{\omega=0}\right)^{-1}$, where $\Sigma_l^{\text{BR}}(\omega)$ and $\Sigma_l^{\text{SH}}(\omega)$ are the self-energies given by breathing and shear phonons, respectively. Since the renormalization due to the self-energy takes place only for $|\omega| < \omega_\alpha$ [28], we approximate $z_l(\omega)$ as

$$z_l(\omega) = \begin{cases} \left(1 - \frac{\partial \Sigma_l^{\text{BR}}(\omega)}{\partial \omega} \Big|_{\omega=0} - \frac{\partial \Sigma_l^{\text{SH}}(\omega)}{\partial \omega} \Big|_{\omega=0}\right)^{-1} & (|\omega| < \omega_{\text{SH}}) \\ \left(1 - \frac{\partial \Sigma_l^{\text{BR}}(\omega)}{\partial \omega} \Big|_{\omega=0}\right)^{-1} & (\omega_{\text{SH}} < |\omega| < \omega_{\text{BR}}) \\ 1 & (\omega_{\text{BR}} < |\omega|) \end{cases} \quad (41)$$

Note that T_c is reduced by $z_l(\omega)$. In the one-loop ap-

proximation [28], $\Sigma_l^{\text{BR}}(\omega)$ and $\Sigma_l^{\text{SH}}(\omega)$ are given by

$$\Sigma_{a_{1g}}^{\text{BR}}(i\varepsilon_n) = T \sum_m a_1^2 G_{a_{1g}}(i\varepsilon_n - i\omega_m) D_{\text{BR}}(i\omega_m), \quad (42)$$

$$\Sigma_{e_g}^{\text{BR}}(i\varepsilon_n) = T \sum_m a_2^2 G_{e_g}(i\varepsilon_n - i\omega_m) D_{\text{BR}}(i\omega_m), \quad (43)$$

$$\Sigma_{a_{1g}}^{\text{SH}}(i\varepsilon_n) = T \sum_m 2b_1^2 G_{eg}(i\varepsilon_n - i\omega_m) D_{\text{SH}}(i\omega_m), \quad (44)$$

$$\Sigma_{eg}^{\text{SH}}(i\varepsilon_n) = T \sum_m \left\{ b_1^2 G_{a_{1g}}(i\varepsilon_n - i\omega_m) + 2b_2^2 G_{eg}(i\varepsilon_n - i\omega_m) \right\} D_{\text{SH}}(i\omega_m). \quad (45)$$

In deriving above equations, we have put $D_\alpha(i\omega_m) = \frac{2}{\omega_\alpha} \theta(\omega_\alpha - |\omega_m|)$ for simplicity. Then, the differential coefficient of self-energy at $\omega = 0$ is expressed in the following form.

$$-\frac{\partial}{\partial \omega} \left(\begin{array}{c} \Sigma_{a_{1g}}^{\text{BR}}(\omega) \\ \Sigma_{eg'}^{\text{BR}}(\omega) \end{array} \right) \Big|_{\omega=0} = \frac{2}{\pi} \int_{-\infty}^{\infty} \begin{pmatrix} a_1^2 & 0 \\ 0 & a_2^2 \end{pmatrix} \begin{pmatrix} \rho_{a_{1g}}(\varepsilon) \\ \rho_{eg'}(\varepsilon) \end{pmatrix} \frac{1}{\varepsilon^2 + \omega_{\text{BR}}^2} d\varepsilon, \quad (46)$$

$$-\frac{\partial}{\partial \omega} \left(\begin{array}{c} \Sigma_{a_{1g}}^{\text{SH}}(\omega) \\ \Sigma_{eg'}^{\text{SH}}(\omega) \end{array} \right) \Big|_{\omega=0} = \frac{2}{\pi} \int_{-\infty}^{\infty} \begin{pmatrix} 0 & 2b_1^2 \\ b_1^2 & 2b_2^2 \end{pmatrix} \begin{pmatrix} \rho_{a_{1g}}(\varepsilon) \\ \rho_{eg'}(\varepsilon) \end{pmatrix} \frac{1}{\varepsilon^2 + \omega_{\text{SH}}^2} d\varepsilon. \quad (47)$$

In the next section, we solve Eqs. (35)-(36) self-consistently using Eqs. (40)-(41), and obtain T_c that is determined by the condition $\lambda = 1$ in Eq. (35).

IV. NUMERICAL RESULT

Here, we perform numerical study: In calculating T_c , important model parameters are a_1 , b_1 and Δ : a_1 (b_1) represents the EPI due to breathing mode (shear mode) in the a_{1g} -orbital (between a_{1g} - and e'_g -orbitals), and Δ is the energy of the top of the e'_g bands measured from the Fermi level in Fig. 4 (b). Note that $\Delta < 0$ experimentally [15, 17, 18]. The values of a_1 and b_1 obtained in the present paper is slightly larger than those used in Ref. [28]. Therefore, the mass enhancement factors in the present model given by Eqs. (46) and (47) are slightly larger than those in Fig. 2 of Ref. [28]: In the present model, $z_{a_{1g}}^{-1}(0)$ is around 2 for $\Delta \sim -0.02$ eV, and it decreases moderately as Δ decreases.

Then, T_c is obtained by solving the set of gap equations (35)-(36). In the absence of Coulomb interaction, the obtained T_c - Δ phase diagram is qualitatively similar to Fig. 4 in Ref. [28], where obtained T_c is about 10 times higher than the experimental T_c . In this section, we solve the gap equation in the presence of strong Coulomb interaction between d -electrons. We will show that the obtained T_c is reduced to be comparable with experimental T_c by assuming reasonable values of U and J . In the presence of shear phonons ($b_1 \neq 0$), gap function for e'_g orbital $\phi_{eg'}(i\varepsilon_n)$ is finite even if the e'_g bands sink below the Fermi level ($\Delta < 0$). Due to this interband transition of Cooper pairs, which we call the valence band SK effect, s -wave T_c is considerably enhanced.

In Fig. 5, we show U -dependence of T_c at $\Delta = -0.03$ eV for unhydrate ($b_1 = 0.2$ eV and $b_2 = 0.067$ eV) and hydrate ($b_1 = 0.23$ eV and $b_2 = 0.78$ eV) systems, respectively. We see that T_c decrease monotonically with U since the attractive force due to phonons is reduced by U . In the absence of shear phonons ($b_1 = b_2 = 0$), T_c

is independent of Δ . Experimental $T_c \sim 4 \times 10^{-4}$ eV is realized at $U \sim 1.75$ eV, whereas T_c is almost zero for $U \geq 4$ eV. In the presence of both breathing and shear phonons, obtained T_c is considerably enlarged owing to the valence band SK effect induced by shear phonons, which is represented by b_1^2 in Eq. (39). For $U \sim 4$ eV, obtained T_c for hydrate system is more than three times larger than that for unhydrate one. In §V A, we explain the reason why SK effect is strong against large Coulomb interaction.

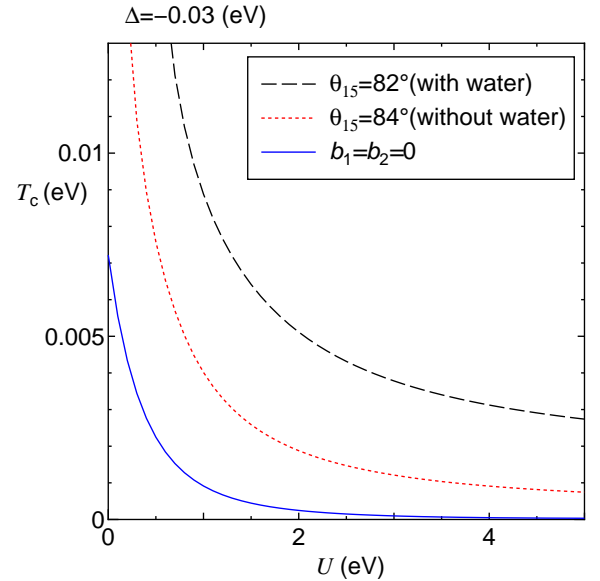


FIG. 5: (Color online) U -dependence of T_c for $\Delta = 0.03$ eV.

In Fig. 6, we show the Δ -dependence of T_c at $U = 4$ and 6 eV for unhydrate and hydrate systems, respectively. Note that the cluster calculation using quantum chemical ab-initio methods suggests $U = 4.1 \sim 4.8$ eV [34]. In both cases, T_c is almost zero if we drop shear phonons ($b_1 = b_2 = 0$). In the presence of shear phonons,

on the other hand, obtained T_c is comparable to or higher than experimental T_c due to the valence band SK effect for $|\Delta| \lesssim \omega_{\text{SH}}$. In Fig. 6, T_c increases monotonically with increasing Δ (< 0) due to SK effect, in particular for $|\Delta| < \omega_{\text{SH}}$. ARPES study in hydrated $\text{Na}_x\text{CoO}_2 \cdot y\text{H}_2\text{O}$ [17] suggests that $\Delta \sim -0.03$ eV, which is closer to the Fermi level than the Debye frequency of shear phonon $\omega_{\text{SH}} = 480 \text{ cm}^{-1} \sim 0.06$ eV. On the other hand, ARPES studies in unhydrated Na_xCoO_2 [15, 18] suggest $\Delta \sim -0.1$ eV. Therefore, our results are consistent with these experimental results.

The theoretical value of T_c in Fig. 6 for $|\Delta| \sim 0.02 - 0.03$ eV is much larger than experimental T_c , even for parameters of “without water”. Therefore, we also calculate T_c for smaller values of b_1 and b_2 in Fig. 6; $b_1 = 0.18$ eV and $b_2 = 0.062$ eV. The obtained T_c for $|\Delta| \sim 0.02 - 0.03$ eV is comparable with experimental value $T_c = 5\text{K} \approx 0.04$ eV.

In Appendix, we analytically study the transition temperature by taking account of the valence band SK effect. The obtained expression for T_c is given in Eq. (A14), where the effective coupling constant λ_{eff} is given in Eq. (A15). Since $\lambda_2, \lambda_3 \propto b_1$, the second term in Eq. (A15) represents the contribution due to the valence band SK effect. This term increases as Δ approaches zero since λ_{Δ} is a decrease function of Δ (< 0).

Finally, we summarize the results of this section. Owing to the valence band SK effect, the obtained s -wave T_c is relatively high even if we take account of the realistic Coulomb repulsion $U = 4 \sim 6$ eV. Moreover, not only Δ approaches zero but also EPI for shear phonons (b_1 and b_2) increase due to the change of crystal structure by water intercalation, as explained in §II B. For this reason, s -wave superconductivity is realized against strong Coulomb interaction in hydrated $\text{Na}_x\text{CoO}_2 \cdot y\text{H}_2\text{O}$.

V. DISCUSSION

A. Why SK mechanism can overcome strong Coulomb interaction?

In §IV, we have shown that T_c becomes 0 at relatively small U (~ 4 eV) when we consider only breathing phonon, while large T_c is realized even for $U \geq 4$ eV when we consider shear phonons as well as breathing phonon. This result indicates that the SK mechanism is suppressed by the Coulomb interactions only slightly. In fact, the attractive force due to shear phonons is reduced by $J \sim U/10$, which means that the reduction of the SK mechanism due to Coulomb interaction is very small. Moreover, J is prominently reduced by the retardation effect, as we will explain below:

In a single band model, the retardation effect was discussed by Morel and Anderson [45]. In Appendix, we extend their theory to the multi-band model for Na_xCoO_2 . The renormalized Coulomb interactions are obtained by solving set of equations (A7)-(A10). Here, we approxi-

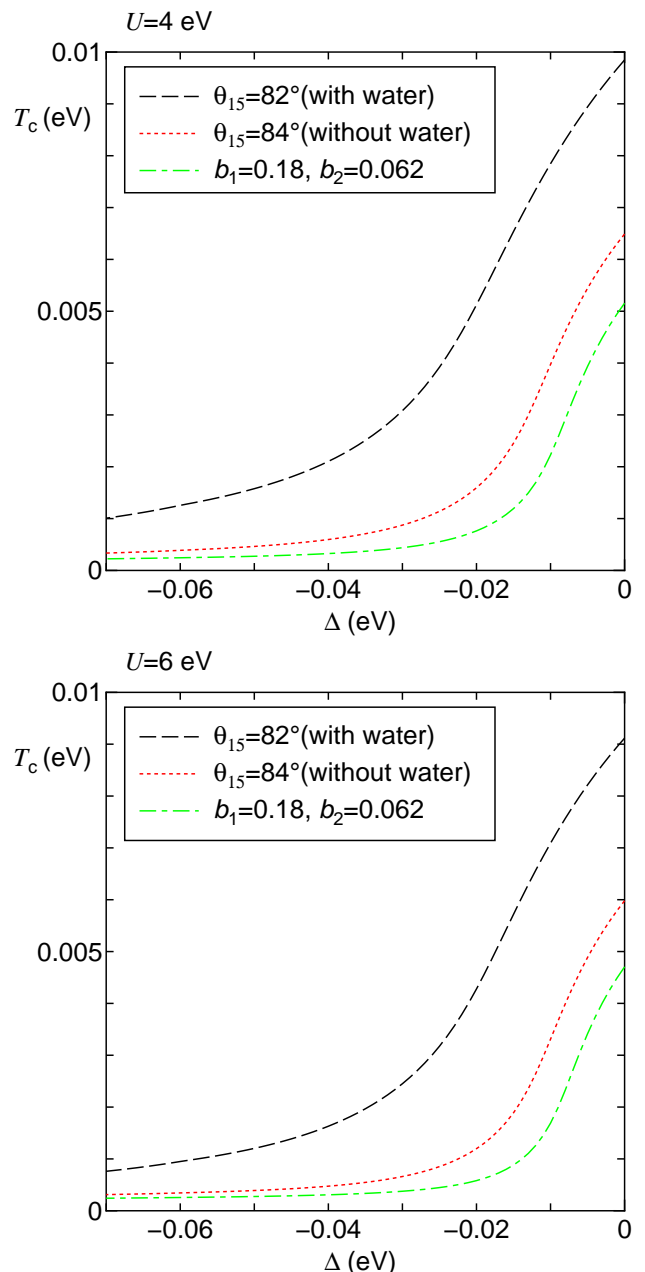


FIG. 6: (Color online) Δ -dependence of T_c at $U=4$ eV (top) and $U=6$ eV (bottom). The dashed and dotted line represent T_c for hydrated $\text{Na}_x\text{CoO}_2 \cdot y\text{H}_2\text{O}$ ($b_1 = 0.223, b_2 = 0.0775$) and unhydrated Na_xCoO_2 ($b_1 = 0.196, b_2 = 0.0665$), respectively.

mate the DOS for the a_{1g} - and e'_g -bands as $\rho_{a_{1g}}(\omega) = \rho_{a_{1g}}\theta(W - |\omega|)$ and $\rho_{e'_g}(\omega) = \rho_{e'_g}\theta(\Delta - \omega)\theta(W + \omega)$ [see Fig. 9 in appendix]. Here, $2W$ is the bandwidth of the a_{1g} -band. In a realistic parameter regime $U \gg J$, these

equations can be solved easily. The obtained results are

$$U_{a1g}^* \approx U/(1 + AU), \quad (48)$$

$$U_{eg'}^* \approx U/(1 + BU), \quad (49)$$

$$J_{a1g,eg'}^* \approx J/(1 + AU)(1 + BU), \quad (50)$$

$$J_{eg',eg'}^* \approx J/(1 + BU)^2, \quad (51)$$

where U_{a1g}^* ($U_{eg'}^*$) is renormalized Coulomb interaction between a_{1g} electrons (e'_g electrons), $J_{a1g,eg'}^*$ ($J_{eg',eg'}^*$) is renormalized pair hopping between a_{1g} and e'_g orbitals (e'_g orbitals). $A = \rho_{a1g} \ln(W/\omega_D)$ and $B = \frac{1}{2}\rho_{eg'} \ln(W/\omega_D)$ are the renormalization factors. In the present model, $A \approx 1.2$ and $B \approx 1.0$ [46]. (Note that $\rho_{a1g}U_{a1g}^*$ ($\rho_{eg'}U_{eg'}^*$) corresponds to Anderson-Morel pseudopotential μ for a single band model.) Since the renormalization factor for J in Eqs. (50) and (51) is square of that for U , J^* becomes very small. In the present model, $U_{a1g}^*/U \approx 1/7$ and $J_{a1g,eg'}^*/J \approx 1/42$ at $U \approx 5$ eV. For this reason, the effect of the Coulomb interactions on the SK mechanism becomes remarkably small. Therefore, in the case of $|\Delta| \ll \omega_D$, s -wave superconducting state is realized owing to the SK effect even in the presence of strong Coulomb interaction.

B. Isotope effect on T_c

Recently, Yokoi et al. studied the isotope effect on T_c in $\text{Na}_x\text{CoO}_2 \cdot y\text{H}_2\text{O}$ by substituting ^{16}O atoms with ^{18}O atoms [47]. They found that the isotope effect coefficient α ($T_c \propto M^{-\alpha}$, where M is the mass of O ion) is considerably smaller than the simple BCS value 0.5. Here, we study the isotope effect on T_c in the present model, and explain that the value of α approaches zero because of the strong Coulomb interaction.

According to the BCS theory, T_c in a single band model is $T_c = 1.13\omega_D e^{-1/\lambda^*}$ and $\lambda^* = 2N(0)a^2/\omega_D - \mu^*$, where $N(0)$ is the density of states, a is the EPI, and $\mu^* = N(0)U/(1 + N(0)U \ln(W/\omega_D))$ is the Anderson-Morel pseudo potential. In the case of $\mu^* = 0$ ($U = 0$), $2N(0)a^2/\omega_D$ is independent of M since $a \propto (M\omega_D)^{-1/2} \propto M^{-1/4}$. Then, $T_c \propto \omega_D \propto M^{-1/2}$ (i.e., $\alpha = 0.5$). However, α becomes smaller than 0.5 in the case of $U > 0$, since μ^* decreases as M ($\propto \omega_D^{-2}$) increases. In fact, $\alpha \sim 0$ in Ru and Zr, both of which are $4d$ -electron s -wave superconductors. Since both $N(0)U$ and ω_D/W are relatively large in $\text{Na}_x\text{CoO}_2 \cdot y\text{H}_2\text{O}$, the value of α is expected to be much smaller than 0.5.

Figure 7 show the obtained isotope effect on T_c at $\Delta = -0.025$ eV and $\Delta = -0.04$ eV, by assuming $\omega_\alpha \propto M^{-1/2}$ and $a_1, a_2, b_1, b_2 \propto M^{-1/4}$. For b_1 and b_2 , we use the smaller values than the estimated ones in Table I to reproduce the experimental T_c (~ 4.5 K). We use $b_1 = 0.18$ eV, $b_2 = 0.062$ eV for $\Delta = -0.025$ eV, and $b_1 = 0.20$ eV, $b_2 = 0.067$ eV for $\Delta = -0.04$ eV. (In both cases, we put $a_1 = 0.22$ eV and $a_2 = 0.25$ eV, which are same with the estimated values in Table II.)

For both parameters, the reduction of T_c due to isotope effect, ΔT_c , decreases with U . We see that ΔT_c becomes almost 0 at $U \sim 5$ eV, and it becomes positive at $U = 6$ eV. Therefore, ΔT_c in Na_xCoO_2 may be too small to probe it experimentally. At $U = 3$ eV, the obtained α is about half of the BCS value ($\alpha = 0.5$). α becomes almost 0 at $U = 5$ eV, and it becomes negative at $U = 6$ eV (inverse isotope effect). Therefore, α approaches zero in $\text{Na}_x\text{CoO}_2 \cdot y\text{H}_2\text{O}$ due to the strong Coulomb interaction, even if the s -wave superconductivity is caused by EPI.

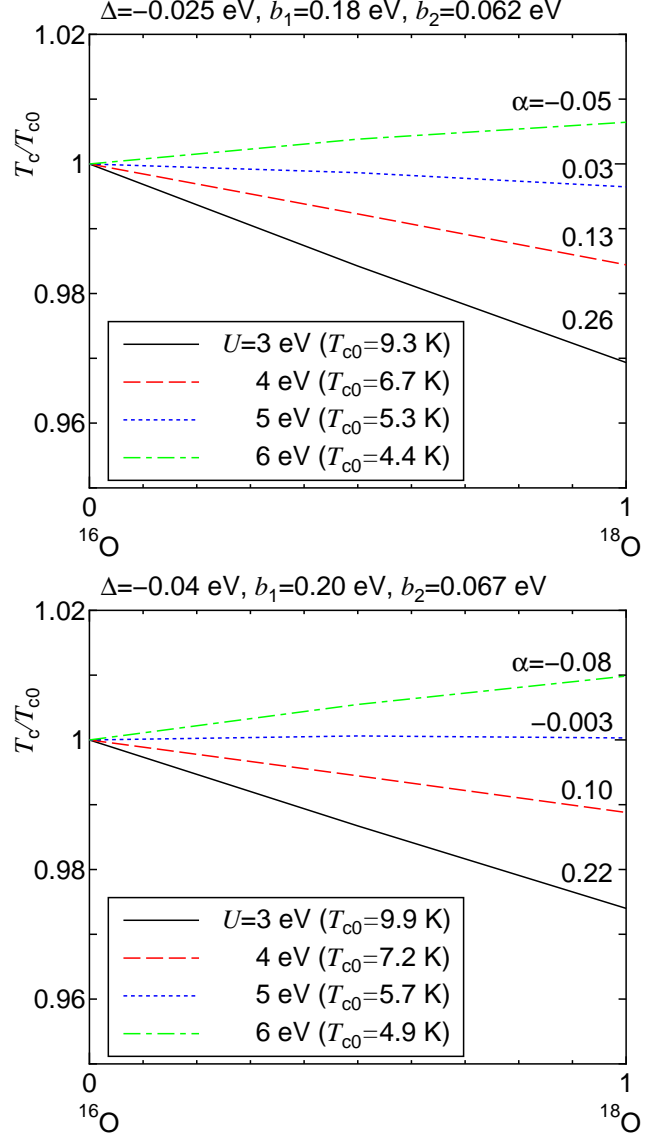


FIG. 7: (Color online) Isotope effect on T_c for at $\Delta = -0.025$ eV, $b_1 = 0.18$ eV, $b_2 = 0.062$ eV (top), and $\Delta = -0.04$ eV, $b_1 = 0.20$ eV, $b_2 = 0.067$ eV (bottom). The lateral axis shows the rate of ^{18}O ions and the longitudinal axis shows T_c/T_{c0} where T_{c0} is T_c for ^{16}O ion. Note that $\alpha = -\partial \ln T_c / \partial \ln M$ is the isotope effect coefficient.

C. Origin of the anisotropy of the superconducting gap

In this paper, we have studied the s -wave superconducting state due to EPI in $\text{Na}_x\text{CoO}_2 \cdot y\text{H}_2\text{O}$. However, the nuclear relaxation ratio $1/T_1$ is proportional to T^3 below T_c , which suggests that the nodal superconducting state is realized [12]. Presence of gap anisotropy is also indicated by the specific heat measurements below T_c [48, 49]. In the present calculation, we have neglected the \mathbf{k} -dependence of the superconducting gap for simplicity. Here, we discuss the possibility of realizing an anisotropic s -wave state in $\text{Na}_x\text{CoO}_2 \cdot y\text{H}_2\text{O}$, resulting from the coexistence of the strong EPI and the AF fluctuations.

In $(\text{Y,Lu})\text{Ni}_2\text{B}_2\text{C}$, strongly anisotropic superconducting state is realized below $T_c \sim 15$ K [50, 51]. The superconducting gap becomes isotropic by introducing small amount of impurities, whereas T_c is almost unchanged [52]. They are hallmarks of anisotropic s -wave superconducting state. According to Ref. [50], the ratio of gap anisotropy reaches $\Delta_{\max}/\Delta_{\min} \sim 10$ in a clean sample. Recently, one of the authors of this paper had studied the mechanism of this anisotropic s -wave superconductivity [53]: By solving the strong coupling Eliashberg equation, he found that the s -wave superconducting gap due to the EPI can be strongly anisotropic even in a single FS model, if strong AF fluctuations exist. In this case, pairs of gap minima appear at points on the FS which are connected by the nesting vector \mathbf{Q} . In the normal state of $\text{Na}_x\text{CoO}_2 \cdot y\text{H}_2\text{O}$, prominent AF fluctuations had been observed by $1/T_1$ measurements [12, 54]. According to Ref. [54], $\text{Na}_x\text{CoO}_2 \cdot y\text{H}_2\text{O}$ locates in the close vicinity of the AF quantum critical point. Recent neutron diffraction measurement reports that the wavevector of the AF fluctuations is $\mathbf{Q}_2 = \overline{\Gamma\text{M}} = (0, 2\pi/\sqrt{3})$ and $(\pi, \pm\pi/\sqrt{3})$ [55].

According to the study using the FLEX approximation [19], there are two candidates for the nesting vectors in Na_xCoO_2 for $\Delta < 0$. One is $\mathbf{Q}_1 = \overline{\Gamma\text{K}} = (4\pi/3, 0)$ and $(\pm 2\pi/3, 2\pi/\sqrt{3})$ that originates from the a_{1g} large FS around Γ -point. The another one is \mathbf{Q}_2 that originates from the nesting of e'_g hole pockets near K-points. Note that the AF fluctuations with \mathbf{Q}_2 appear when the top of the e'_g bands is very close to Fermi level [19]. When the hole number is 0.65, which corresponds to the hole number of $\text{Na}_{0.35}\text{CoO}_2 \cdot 1.3\text{H}_2\text{O}$ without oxonium ion, the resultant minimum gap points are shown in Fig 8 (a), when the wavenumber of AF fluctuations is either \mathbf{Q}_1 or \mathbf{Q}_2 . Note that the sign of the gap function is the same everywhere. On the other hand, when the hole number is about 0.5, which can be realized in the presence of oxonium ion as a substitute for water molecule [35], the resultant minimum gap points are shown in Fig 8 (b) when the wavenumber of AF fluctuations is \mathbf{Q}_2 . In both cases, anisotropic s -wave superconductivity is realized in the e'_g -band FS in $\text{Na}_x\text{CoO}_2 \cdot y\text{H}_2\text{O}$.

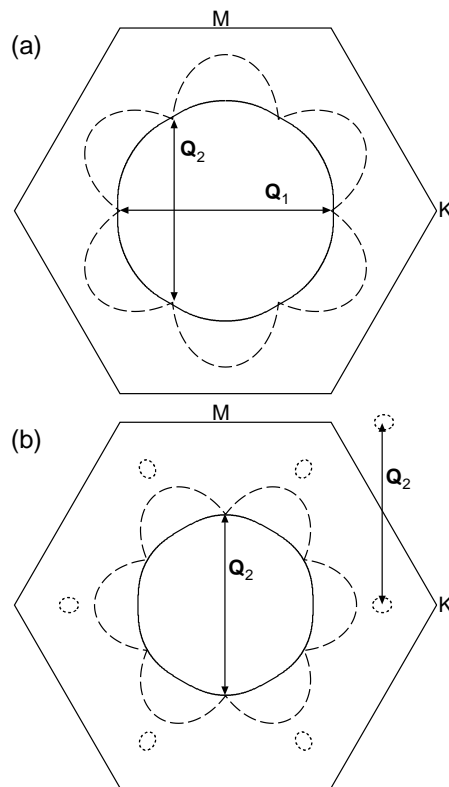


FIG. 8: Expected anisotropic s -wave superconducting gap for (a) $n_h \sim 0.65$ and (b) $n_h \sim 0.5$, where n_h is the hole number of t_{2g} orbital. The dashed lines represent the magnitude of gap function, whose sign is positive everywhere. Tops of the e'_g -bands, which are just below the Fermi level, are shown by dotted lines in (b).

In Ref. [53], we have shown that the relation $1/T_1 \propto T^3$ below T_c can be realized in the anisotropic s -wave state under the influence of strong AF fluctuations. Moreover, we have recently verified that the two-gap type specific heat observed in Refs. [48, 49] can be realized in this anisotropic s -wave state, by considering only the a_{1g} FS [56]. It is an important future problem to reproduce the anisotropic s -wave state microscopically based on the d - p Holstein Hubbard model for Na_xCoO_2 .

VI. SUMMARY

In Na_xCoO_2 , existence of the strong EPI is suggested by ARPES measurements [16], and the absence of impurity effect on T_c strongly indicates the realization of the s -wave superconducting state without sign change of the gap function. In the present paper, we have studied the electron-phonon mechanism of superconductivity by considering two relevant optical phonon modes (breathing and shear phonons), and found that strong pairing interaction is caused by the interband hopping of Cooper pairs induced by shear phonons. This mechanism is im-

portant even if the top of e'_g electron band is close to but below the Fermi level as suggested experimentally. Therefore, this valence-band SK mechanism is the origin of s -wave superconductivity in Na_xCoO_2 , overcoming the strong Coulomb interaction $U \sim 5$ eV.

In this paper, we have derived the EPI for breathing and shear phonons by considering both the Coulomb potential and the transfer integrals. The estimated EPI for shear phonon is prominently increased by water intercalation, resulting from the increase of trigonal distortion of CoO_2 layer. According to the point charge model, the top of the e'_g bands $\Delta (< 0)$ is expected to approach the Fermi level due to water intercalation. Both effects induced by the water intercalation will raise T_c due to the SK mechanism.

Based on the obtained model Hamiltonian, we determine T_c by solving the strong coupling Eliashberg equation. The SK mechanism is seldom damaged by the Coulomb interaction since the pair hopping J , which is the depairing force for the SK mechanism, is much smaller than U . For this reason, experimental $T_c \sim 5$ K is realized irrespective of the realistic Coulomb interaction $U \sim 5$ eV. We have also studied the oxygen isotope effect ($^{16}\text{O} \rightarrow ^{18}\text{O}$) on T_c . In the absence of Coulomb interaction, T_c decreases by the isotope substitution in proportion to $\omega_D \propto M_O^{-1/2}$. However, we found that the isotope effect on T_c becomes very small for $U = 4 \sim 6$ eV, since the renormalized Coulomb interaction (Anderson-Morel potential) is reduced with the decrease of ω_D .

Acknowledgments

We are grateful to M. Sato, Y. Kobayashi, M. Yokoi and T. Moyoshi for fruitful discussions on experimental results, including their unpublished data. We are also grateful to G.-q. Zheng, K. Ishida, Y. Ihara, T. Shimojima, H. Sakurai and T. Sato for enlightening discussions on experiments. Finally, we thank D.S. Hirashima, M. Ogata, K. Kuroki, Y. Tanaka, Y. Yanase and M.

Mochizuki for valuable comments and discussions on theoretical issues. This work was supported by the Grant-in-Aid for Scientific Research from the Ministry of Education, Science, Sports and Culture of Japan. Numerical calculations were performed at the supercomputer center, ISSP.

APPENDIX A: ANALYTICAL EXPRESSION FOR THE TRANSITION TEMPERATURE IN $\text{Na}_x\text{CoO}_2 \cdot y\text{H}_2\text{O}$

In this appendix, we derive the analytical expression for s -wave T_c in $\text{Na}_x\text{CoO}_2 \cdot y\text{H}_2\text{O}$. For this purpose, we simplify the model further. Here, we approximate the DOS for the a_{1g} - and e'_g -bands as $\rho_{a_{1g}}(\omega) = \rho_{a_{1g}}\theta(W - |\omega|)$ and $\rho_{e'_g}(\omega) = \rho_{e'_g}\theta(\Delta - \omega)\theta(W + \omega)$, which are shown in Fig. 9. Hereafter, we promise that $\Delta < 0$. We also approximate the phonon Green function by the step function $D(i\omega_m) = \frac{2}{\omega_D}\theta(\omega_D - |\omega_m|)$, and assume that the Debye frequencies of breathing and shear phonon are the same for simplicity ($\omega_D \equiv \omega_{\text{BR}} = \omega_{\text{SH}}$). Then, the gap equation at $T = T_c$ given in Eq. (35) becomes

$$\hat{\phi}(i\varepsilon_n) = T_c \sum_{|\omega_m| \leq \omega_D} \begin{pmatrix} a_1^2 & 2b_1^2 \\ b_1^2 & a_2^2 + 2b_2^2 \end{pmatrix} \frac{2}{\omega_D} \hat{F}(i\varepsilon_n - i\omega_m) - T_c \sum_{\omega_m} \begin{pmatrix} U & 2J \\ J & U + J \end{pmatrix} \hat{F}(i\varepsilon_n - i\omega_m), \quad (\text{A1})$$

Here, we assume that $\hat{\phi}(i\varepsilon_n)$ is given by the step function

$$\hat{\phi}(i\varepsilon_n) = \begin{cases} \hat{\phi}^{\text{I}} & (|\varepsilon_n| < \omega_D) \\ \hat{\phi}^{\text{II}} & (|\varepsilon_n| > \omega_D) \end{cases}. \quad (\text{A2})$$

First, we consider the case of $|\varepsilon_n| \ll \omega_D$. Then, the gap equation for $\hat{\phi}^{\text{I}}$ is obtained from Eq. (A1).

$$\hat{\phi}^{\text{I}} = \left[\begin{pmatrix} a_1^2 & 2b_1^2 \\ b_1^2 & a_2^2 + 2b_2^2 \end{pmatrix} \frac{2}{\omega_D} - \begin{pmatrix} U & 2J \\ J & U + J \end{pmatrix} \right] \left(\frac{\sum^{\text{I}} |G_{a_{1g}}(\mathbf{k}, i\varepsilon_\ell)|^2 \phi_{a_{1g}}^{\text{I}}}{\sum^{\text{I}} |G_{e'_g}(\mathbf{k}, i\varepsilon_\ell)|^2 \phi_{e'_g}^{\text{I}}} \right) - \begin{pmatrix} U & 2J \\ J & U + J \end{pmatrix} \left(\frac{\sum^{\text{II}} |G_{a_{1g}}(\mathbf{k}, i\varepsilon_\ell)|^2 \phi_{a_{1g}}^{\text{II}}}{\sum^{\text{II}} |G_{e'_g}(\mathbf{k}, i\varepsilon_\ell)|^2 \phi_{e'_g}^{\text{II}}} \right), \quad (\text{A3})$$

where \sum^{I} and \sum^{II} represent $\frac{T_c}{N} \sum_{\mathbf{k}} \sum_{|\varepsilon_\ell| \leq \omega_D}$ and $\frac{T_c}{N} \sum_{\mathbf{k}} \sum_{|\varepsilon_\ell| > \omega_D}$, respectively. Next, we consider the case of $|\varepsilon_n| \gg \omega_D$, where $F(i\varepsilon_n - i\omega_m) \propto (\phi_{a_{1g}}^{\text{II}}, \phi_{e'_g}^{\text{II}})$ for

$|\omega_m| \leq \omega_D$. Then, the gap equation for $\hat{\phi}^{\text{II}}$ is given by

$$\hat{\phi}^{\text{II}} \simeq - \begin{pmatrix} U & 2J \\ J & U + J \end{pmatrix} \left(\frac{\sum^{\text{II}} |G_{a_{1g}}(\mathbf{k}, i\varepsilon_\ell)|^2 \phi_{a_{1g}}^{\text{II}}}{\sum^{\text{II}} |G_{e'_g}(\mathbf{k}, i\varepsilon_\ell)|^2 \phi_{e'_g}^{\text{II}}} \right) - \begin{pmatrix} U & 2J \\ J & U + J \end{pmatrix} \left(\frac{\sum^{\text{I}} |G_{a_{1g}}(\mathbf{k}, i\varepsilon_\ell)|^2 \phi_{a_{1g}}^{\text{I}}}{\sum^{\text{I}} |G_{e'_g}(\mathbf{k}, i\varepsilon_\ell)|^2 \phi_{e'_g}^{\text{I}}} \right). \quad (\text{A4})$$

Here, we ignored the phonon contribution that is proportional to ϕ^{II} , since it is much smaller than the first term in Eq. (A4).

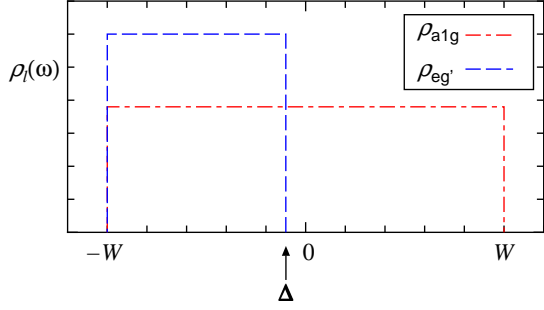


FIG. 9: (Color online) The simplified DOS for the a_{1g} - and e'_g -bands.

Using eq. (A4), $\hat{\phi}^{\text{II}}$ in Eq. (A3) can be eliminated. Then, the obtained gap equation for $\hat{\phi}^{\text{I}}$ is given by

$$\hat{\phi}^{\text{I}} = \hat{V}_{\text{eff}}^* \left(\frac{\sum^{\text{I}} |G_{a_{1g}}(\mathbf{k}, i\varepsilon_\ell)|^2 \phi_{a_{1g}}^{\text{I}}}{\sum^{\text{I}} |G_{e'_g}(\mathbf{k}, i\varepsilon_\ell)|^2 \phi_{e'_g}^{\text{I}}} \right), \quad (\text{A5})$$

$$V_{\text{eff}}^* = \begin{pmatrix} a_1^2 & 2b_1^2 \\ b_1^2 & a_2^2 + 2b_2^2 \end{pmatrix} \frac{2}{\omega_{\text{D}}} - \begin{pmatrix} U_{a_{1g}}^* & 2J_{a_{1g}, e'_g}^* \\ J_{a_{1g}, e'_g}^* & U_{e'_g}^* + J_{e'_g, e'_g}^* \end{pmatrix}, \quad (\text{A6})$$

where \hat{V}_{eff}^* is the renormalized effective interaction. $U_{a_{1g}}^*$ ($U_{e'_g}^*$) is the renormalized Coulomb repulsion for the a_{1g} (e'_g) orbital, and J_{a_{1g}, e'_g}^* ($J_{e'_g, e'_g}^*$) is the renormalized pair hopping between (a_{1g} , e'_g) orbitals (e'_g , e'_g) orbitals. These renormalized Coulomb interactions satisfy the following simultaneous equations [46].

$$U_{a_{1g}}^* = U - UAU_{a_{1g}}^* - 2JB J_{a_{1g}, e'_g}^*, \quad (\text{A7})$$

$$U_{e'_g}^* = U - UBU_{e'_g}^* - JAJ_{a_{1g}, e'_g}^* - JB J_{e'_g, e'_g}^*, \quad (\text{A8})$$

$$J_{a_{1g}, e'_g}^* = J - JBU_{e'_g}^* - UAJ_{a_{1g}, e'_g}^* - JB J_{e'_g, e'_g}^*, \quad (\text{A9})$$

$$J_{e'_g, e'_g}^* = J - JBU_{e'_g}^* - JAJ_{a_{1g}, e'_g}^* - UB J_{e'_g, e'_g}^*, \quad (\text{A10})$$

where $A = \sum^{\text{II}} |G_{a_{1g}}(\mathbf{k}, i\varepsilon_\ell)|^2$ and $B = \sum^{\text{II}} |G_{e'_g}(\mathbf{k}, i\varepsilon_\ell)|^2$. If we assume $|\Delta| \ll \omega_{\text{D}}$, then $A = \rho_{a_{1g}} \ln(W/\omega_{\text{D}})$ and $B = \rho_{e'_g} \int_{-\omega_{\text{D}}}^W \frac{1}{\varepsilon} \left(\frac{1}{2} + \frac{1}{\pi} \text{Arctan}\left(\frac{\Delta}{\varepsilon}\right) \right) d\varepsilon \approx \frac{1}{2} \rho_{e'_g} \ln(W/\omega_{\text{D}})$.

We now calculate T_c from Eq. (A5). In the case of $|\Delta| \ll \omega_{\text{D}} \ll W$, $\sum^{\text{I}} |G_\ell(\mathbf{k}, i\varepsilon_n)|^2$ is approximated as follows.

$$\begin{aligned} & \frac{T_c}{N} \sum_{\mathbf{k}} \sum_{|\varepsilon_n| < \omega_{\text{D}}} |G_{a_{1g}}(\mathbf{k}, i\varepsilon_n)|^2 \\ & \simeq T_c \sum_{|\varepsilon_n| < \omega_{\text{D}}} \int_{-\infty}^{\infty} \frac{z_{a_{1g}} \rho_{a_{1g}}}{\varepsilon_n^2 + E^2} dE \\ & = z_{a_{1g}} \rho_{a_{1g}} T_c \sum_{|\varepsilon_n| < \omega_{\text{D}}} \frac{\pi}{|\varepsilon_n|} \\ & \simeq z_{a_{1g}} \rho_{a_{1g}} \ln\left(\frac{1.13\omega_{\text{D}}}{T_c}\right). \end{aligned} \quad (\text{A11})$$

$$\begin{aligned} & \frac{T_c}{N} \sum_{\mathbf{k}} \sum_{|\varepsilon_n| < \omega_{\text{D}}} |G_{e'_g}(\mathbf{k}, i\varepsilon_n)|^2 \\ & \simeq T_c \sum_{|\varepsilon_n| < \omega_{\text{D}}} \int_{-\infty}^{\Delta} \frac{z_{e'_g} \rho_{e'_g}}{\varepsilon_n^2 + E^2} dE \\ & = z_{e'_g} \rho_{e'_g} T_c \sum_{|\varepsilon_n| < \omega_{\text{D}}} \frac{\pi}{|\varepsilon_n|} \left(\frac{1}{2} + \frac{1}{\pi} \text{Arctan}\left(\frac{\Delta}{|\varepsilon_n|}\right) \right) \\ & \simeq \rho_{e'_g} z_{e'_g} \left(\frac{|\Delta|}{\pi\omega_{\text{D}}} + \frac{1}{2} \ln\left(\frac{\omega_{\text{D}}}{|\Delta|}\right) \right). \end{aligned} \quad (\text{A12})$$

As a result, according to Eq. (A5), the equation for T_c is obtained as

$$\frac{\left(\lambda_1^* \ln \frac{1.13\omega_{\text{D}}}{T_c} + \frac{\lambda_4^*}{\lambda_\Delta} \right) + \sqrt{\left(\lambda_1^* \ln \frac{1.13\omega_{\text{D}}}{T_c} - \frac{\lambda_4^*}{\lambda_\Delta} \right)^2 + \frac{4\lambda_2^* \lambda_3^*}{\lambda_\Delta} \ln \frac{1.13\omega_{\text{D}}}{T_c}}}{2} = 1, \quad (\text{A13})$$

where $\lambda_1^* = \left(\frac{2a_1^2}{\omega_{\text{D}}} - U_{a_{1g}}^* \right) z_{a_{1g}} \rho_{a_{1g}}$, $\lambda_2^* = \left(\frac{4b_1^2}{\omega_{\text{D}}} - 2J_{a_{1g}, e'_g}^* \right) z_{e'_g} \rho_{e'_g}$, $\lambda_3^* = \left(\frac{2b_1^2}{\omega_{\text{D}}} - J_{a_{1g}, e'_g}^* \right) z_{a_{1g}} \rho_{a_{1g}}$, $\lambda_4^* = \left(\frac{2(a_2^2 + 2b_2^2)}{\omega_{\text{D}}} - U_{e'_g}^* - J_{e'_g, e'_g}^* \right) z_{e'_g} \rho_{e'_g}$ and $\lambda_\Delta = \left(\frac{|\Delta|}{\pi\omega_{\text{D}}} + \frac{1}{2} \ln\left(\frac{\omega_{\text{D}}}{|\Delta|}\right) \right)^{-1}$.

By solving eq. (A13), T_c is given by

$$T_c = 1.13\omega_{\text{D}} \exp\left(-\frac{1}{\lambda_{\text{eff}}}\right), \quad (\text{A14})$$

$$\lambda_{\text{eff}} = \lambda_1^* + \frac{\lambda_2^* \lambda_3^*}{\lambda_\Delta - \lambda_4^*}. \quad (\text{A15})$$

In Eq. (A15), the first term originates from breathing phonon, and the second term originates from valence

band SK effect. λ_{Δ} monotonically decreases with increasing Δ . Therefore, T_c increase as the top of the e'_g band

approaches the Fermi level.

-
- [1] K. Takada, H. Sakurai, E. Takayama-Muromachi, F. Izumi, R. A. Dilanian and T. Sasaki: *Nature* **422** (2003) 53.
- [2] M. L. Foo, Y. Wang, S. Watauchi, H. W. Zandbergen, T. He, R. J. Cava and N. P. Ong: *Phys. Rev. Lett.* **92** (2004) 247001.
- [3] M. Yokoi, T. Moyoshi, Y. Kobayashi, M. Soda, Y. Yasui, M. Sato and K. Kakurai: *J. Phys. Soc. Jpn.* **74** (2005) 3046.
- [4] D. Yoshizumi, Y. Muraoka, Y. Okamoto, Y. Kiuchi, J. Yamaura, M. Mochizuki, M. Ogata and Z. Hiroi: *J. Phys. Soc. Jpn.* **76** (2007) 063705.
- [5] T. Shimojima, T. Yokoya, T. Kiss, A. Chainani, S. Shin, T. Togashi, S. Watanabe, C. Zhang, C. T. Chen, K. Takada, T. Sasaki, H. Sakurai and E. Takayama-Muromachi: *Phys. Rev. B* **71** (2005) 020505(R).
- [6] D. Wu, J. L. Luo and N. L. Wang: *Phys. Rev. B* **73** (2006) 014523.
- [7] Y. Kobayashi, H. Watanabe, M. Yokoi, T. Moyoshi, Y. Mori and M. Sato: *J. Phys. Soc. Jpn.* **74** (2005) 1800.
- [8] Y. Kobayashi, T. Moyoshi, H. Watanabe, M. Yokoi and M. Sato: *J. Phys. Soc. Jpn.* **75** (2006) 074717.
- [9] G.-q. Zheng, K. Matano, D. P. Chen and C. T. Lin: *Phys. Rev. B* **73** (2006) 180503(R).
- [10] T. Fujimoto, G.-q. Zheng, Y. Kitaoka, R. L. Meng, J. Cmaidalka and C.W. Chu: *Phys. Rev. Lett.* **92** (2004) 047004.
- [11] K. Ishida, Y. Ihara, Y. Maeno, C. Michioka, M. Kato, K. Yoshimura, K. Takada, T. Sasaki, H. Sakurai and E. Takayama-Muromachi: *J. Phys. Soc. Jpn.* **72** (2003) 3041.
- [12] G.-q. Zheng, K. Matano, R. L. Meng, J. Cmaidalka and C. W. Chu: *J. Phys.: Condens. Matter* **18** (2006) L63.
- [13] M. Yokoi, H. Watanabe, Y. Mori, T. Moyoshi, Y. Kobayashi and M. Sato: *J. Phys. Soc. Jpn.* **73** (2004) 1297.
- [14] D. J. Singh: *Phys. Rev. B* **61** (2000) 13397.
- [15] H.-B. Yang, Z.-H. Pan, A. K. P. Sekharan, T. Sato, S. Souma, T. Takahashi, R. Jin, B. C. Sales, D. Mandrus, A. V. Fedorov, Z. Wang and H. Ding: *Phys. Rev. Lett.* **95** (2005) 146401.
- [16] T. Arakane, T. Sato, T. Takahashi, H. Ding, T. Fujii and Atsushi Asamitsu: *J. Phys. Soc. Jpn.* **76** (2007) 054704.
- [17] T. Shimojima, K. Ishizaka, S. Tsuda, T. Kiss, T. Yokoya, A. Chainani, S. Shin, P. Badica, K. Yamada and K. Togano: *Phys. Rev. Lett.* **97** (2006) 267003.
- [18] D. Qian, L. Wray, D. Hsieh, L. Viciu, R. J. Cava, J. L. Luo, D. Wu, N. L. Wang, and M. Z. Hasan: *Phys. Rev. Lett.* **97** (2006) 186405.
- [19] K. Yada and H. Kontani: *J. Phys. Soc. Jpn.* **74** (2005) 2161.
- [20] O. I. Motrunich and P. A. Lee: *Phys. Rev. B* **70** (2004) 024514.
- [21] G. Baskaran: *Phys. Rev. Lett.* **91** (2003) 097003.
- [22] M. Ogata: *J. Phys.: Condens. Matter* **19** (2007) 145282.
- [23] Y. Nisikawa, H. Ikeda and K. Yamada: *J. Phys. Soc. Jpn.* **73** (2004) 1127.
- [24] Y. Yanase, M. Mochizuki and M. Ogata: *J. Phys. Soc. Jpn.* **74** (2005) 430.
- [25] M. Mochizuki, Y. Yanase and M. Ogata: *Phys. Rev. Lett.* **94** (2005) 147005.
- [26] K. Kuroki, S. Onari, Y. Tanaka, R. Arita and T. Nojima: *Phys. Rev. B* **73** (2006) 184503.
- [27] T. Moyoshi, Y. Yasui, M. Soda, Y. Kobayashi, M. Sato and K. Kakurai: *J. Phys. Soc. Jpn.* **75** (2006) 074705.
- [28] K. Yada and H. Kontani: *J. Phys. Soc. Jpn.* **75** (2006) 033705.
- [29] H. Suhl, B. T. Matthias, and L. R. Walker: *Phys. Rev. Lett.* **3** (1959) 552; J. Kondo: *Prog. Theor. Phys.* **29** (1963) 1.
- [30] W. Koshibae and S. Maekawa: *Phys. Rev. Lett.* **91** (2003) 257003.
- [31] W. B. Wu, D. J. Huang, J. Okamoto, A. Tanaka, H.-J. Lin, F. C. Chou, A. Fujimori and C. T. Chen: *Phys. Rev. Lett.* **94** (2005) 146402.
- [32] K. Kuroki, S. Onari, Y. Tanaka, R. Arita and T. Nojima: *Phys. Rev. B* **73** (2006) 184503.
- [33] M. Mochizuki and M. Ogata: *J. Phys. Soc. Jpn.* **76** (2007) 013704.
- [34] S. Landron and M.-B. Lepetit: *cond-mat/0605454*.
- [35] H. Sakurai, N. Tsujii, O. Suzuki, H. Kitazawa, G. Kido, K. Takada, T. Sasaki and E. Takayama-Muromachi: *Phys. Rev. B* **74** (2006) 092502.
- [36] Z. Li, J. Yang, J. G. Hou and Q. Zhu: *Phys. Rev. B* **70** (2004) 144518.
- [37] W. A. Harrison: *Elementary Electronic Structure* (World Scientific, 1999, Singapore).
- [38] J. C. Slater and G. F. Koster: *Phys. Rev.* **94** (1954) 1498.
- [39] J. W. Lynn, Q. Huang, C. M. Brown, V. L. Miller, M. L. Foo, R. E. Schaak, C. Y. Jones, E. A. Mackey and R. J. Cava: *Phys. Rev. B* **68** (2003) 214516.
- [40] *e.g.*, R.D. Shannon and C.T. Prewitt, *Acta Crystallogr. B* **25**, 925 (1969).
- [41] P. Lemmens, K. Y. Choi, V. Gnezdilov, E. Ya. Sherman, D. P. Chen, C. T. Lin, F. C. Chou and B. Keimer: *Phys. Rev. Lett.* **96** (2006) 167204.
- [42] S. Zhou, M. Gao, H. Ding, P. A. Lee and Z. Wang: *Phys. Rev. Lett.* **94** (2005) 206401.
- [43] H. Ishida, M. D. Johannes and A. Liebsch: *Phys. Rev. Lett.* **94** (2005) 196401.
- [44] C. A. Marianetti, K. Haule and O. Parcollet: *Phys. Rev. Lett.* **99** (2007) 246404.
- [45] P. Morel and P. W. Anderson: *Phys. Rev.* **125** (1962) 1263.
- [46] K. Yada and H. Kontani: *Journal of Magnetism and Magnetic Materials* **310** (2007) 684.
- [47] M. Yokoi, Y. Kobayashi and M. Sato: unpublished.
- [48] H. D. Yang, J.-Y. Lin, C. P. Sun, Y. C. Kang, C. L. Huang, K. Takada, T. Sasaki, H. Sakurai and E. Takayama-Muromachi: *Phys. Rev. B* **71** (2005) 020504(R).
- [49] N. Oeschler, R. A. Fisher, N. E. Phillips, J. E. Gordon, M.-L. Foo and R. J. Cava: *cond-mat/0503690*.
- [50] K. Izawa, K. Kamata, Y. Nakajima, Y. Matsuda, T.

- Watanabe, N. Nohara, H. Takagi, P. Thalmeier, and K. Maki, Phys. Rev. Lett. **89**, 137006 (2002).
- [51] T. Watanabe, M. Nohara, T. Hanaguri and H. Takagi: Phys. Rev. Lett **92** (2004) 147002.
- [52] M. Nohara, M. Isshiki, F. Sakai and H. Takagi: J. Phys. Soc. Jpn **68** (1999) 1078.
- [53] H. Kontani: Phys. Rev. B 70 (2004) 054507.
- [54] Y. Ihara, H. Takeya, K. Ishida, H. Ikeda, C. Michioka, K. Yoshimura, K. Takada, T. Sasaki, H. Sakurai and E. Takaayama-Muromachi: J. Phys. Soc. Jpn. 75 (2006) 124714.
- [55] T. Moyoshi and M. Sato, private communication.
- [56] present authors, unpublished.